PNAS

Supporting Information for

The global RNA-RNA interactome of *Klebsiella pneumoniae* unveils a small RNA regulator of cell division

Eric Ruhland, Malte Siemers, Ruman Gerst, Felix Späth, Laura Nicole Vogt, Marc Thilo Figge, Kai Papenfort, Kathrin Sophie Fröhlich

corresponding author: Kathrin Sophie Fröhlich

Email: kathrin.froehlich@uni-jena.de

This PDF file includes:

Supplementary Figure S1

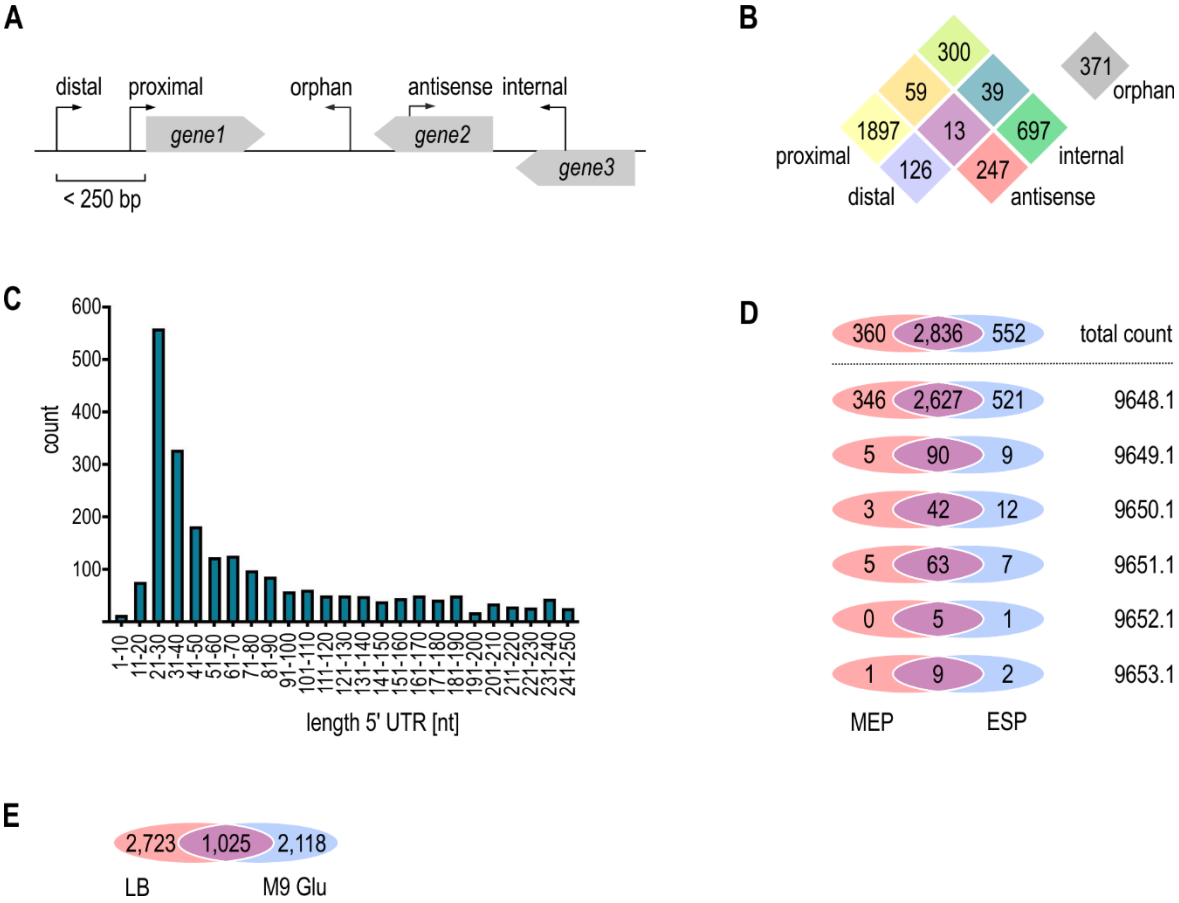

Annotation and classification of transcriptional start sites (TSSs) in *K. pneumoniae* MGH 78578. (A) TSSs were categorized according to their genomic positions. Proximal and distal TSSs are associated with a gene if located ≤ 250 bp upstream of the start codon on the same strand. Antisense TSSs are located on the opposite strand of an annotated gene, internal TSSs within an annotated gene on the sense strand. A TSS not assigned to any of these categories is classified as orphan. (B) Distribution and overlap of classification for 3,748 TSSs identified in this study. (C) Distribution of the lengths of 5' UTRs based on proximal and distal TSSs. (D) Overlap (purple) among TSSs detected in MEP (red) and ESP (blue) distributed between the core genome (9648.1) and the five plasmids (9649.1; 9650.1; 9651.1; 9652.1; 9653.1) in *K. pneumoniae* MGH 78578. (E) Overlap (purple) among TSSs detected in *K. pneumoniae* MGH 78578 in this study for cells grown in LB (red) or in (1) for cells cultivated in minimal M9 medium supplemented with glucose (blue).

Supplementary Figure S2

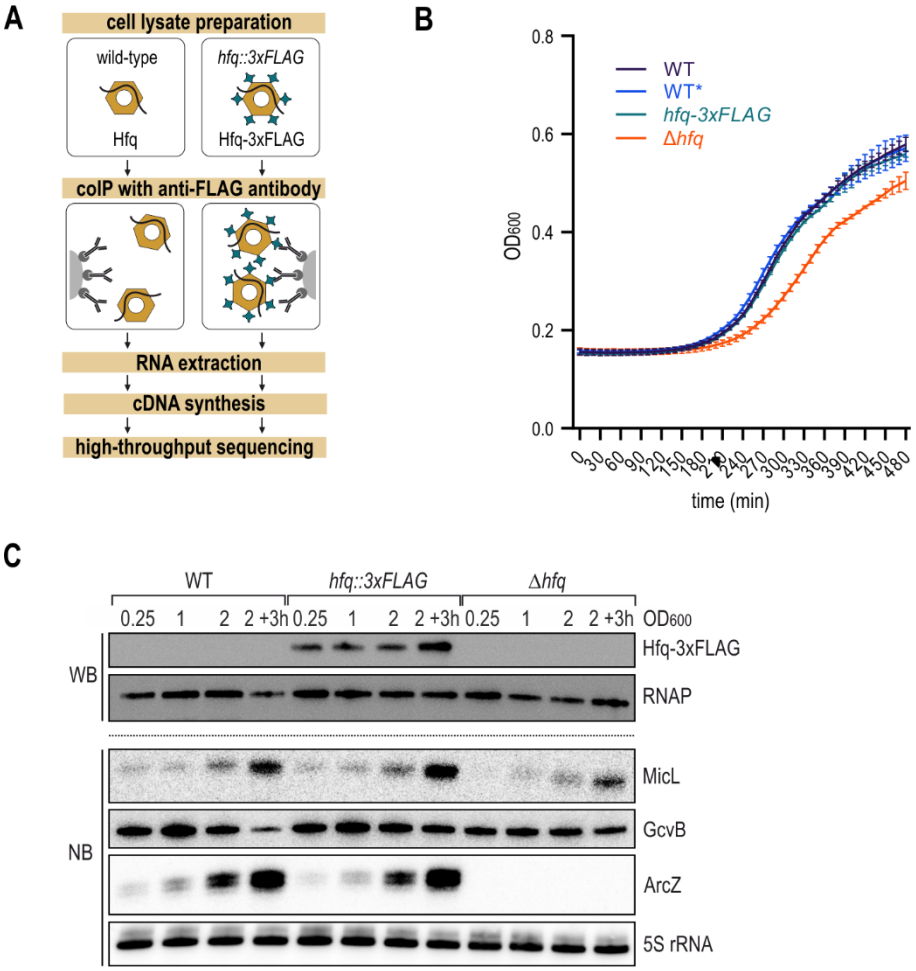

RNA co-immunoprecipitation and expression profiles of *K. pneumoniae*. (A) Strategy to identify Hfq-associated RNA. RNA was co-immunoprecipitated from *K. pneumoniae* (wild-type or chromosomal *hfq::3xFLAG*) using an anti-FLAG antibody. RNA was purified, converted to cDNA, and subjected to high-throughput sequencing. (B) Growth curve of different *K. pneumoniae* strains (wild-type with [WT] or without [WT*] plasmids pKpn4 and pKpn6; chromosomal mutant *hfq::3xFLAG*; chromosomal mutant Δ*hfq*) grown in LB medium. (C) Expression analysis of Hfq-3xFLAG and conserved Hfq-dependent sRNAs. WT and mutant cells (*hfq::3xFLAG* and Δ*hfq*) were grown in LB. Total protein and total RNA samples were collected at indicated optical densities (0.25 to 2 and 3h after cells reached OD_{600} of 2) and subjected to analysis via Western blotting (WB; upper panel) and Northern blotting (NB; lower panel), respectively. RNAP and 5S rRNA served as loading controls.

Supplementary Figure S3

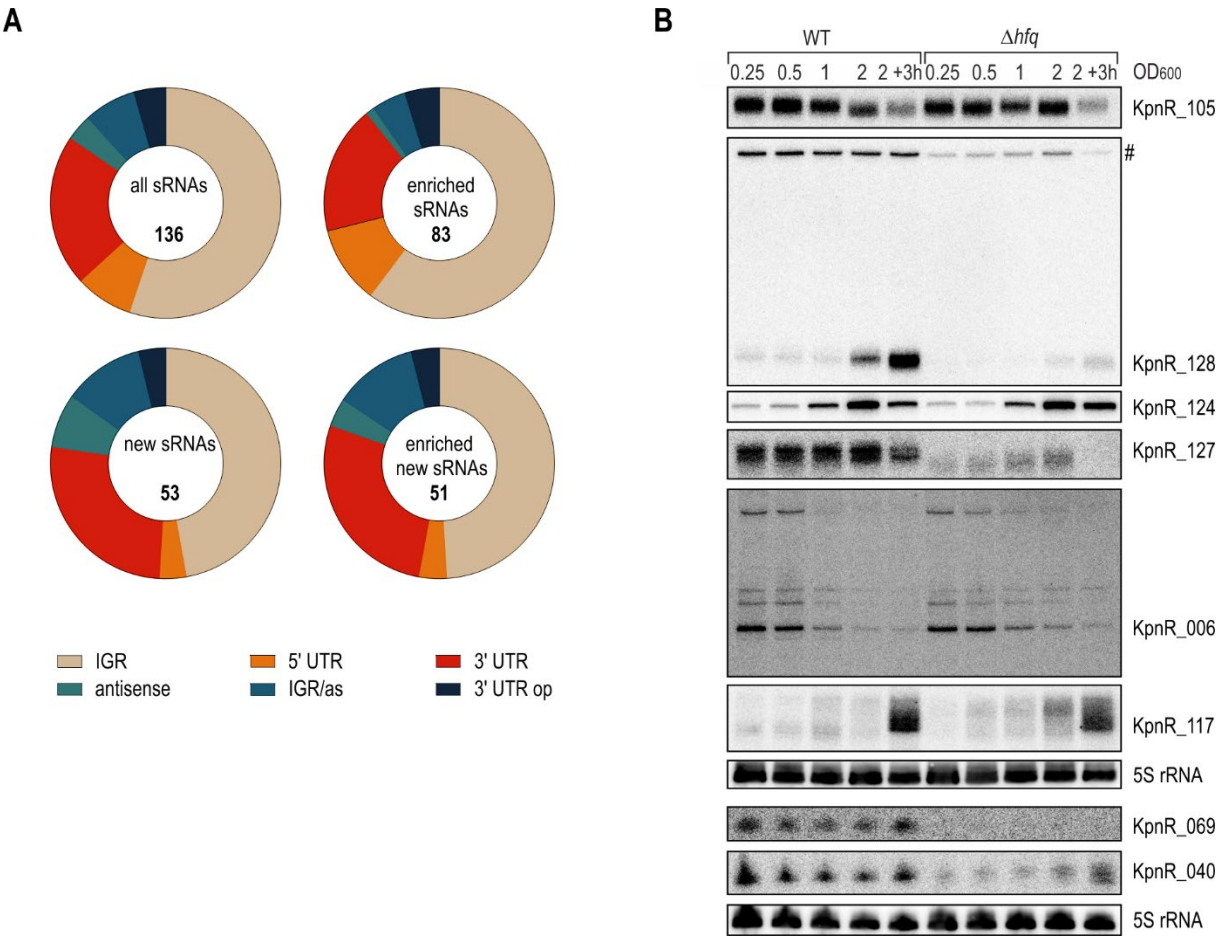

RIP-seq analysis of Hfq-bound sRNAs and expression profiles of selected sRNA candidates. (A) Relative distribution of different sRNA types annotated in *K. pneumoniae* (left), and distribution of different sRNA types enriched ≥3-fold in the co-IP sample compared to the WT control (right). sRNAs are categorized by their genomic location (IGR: free-standing sRNA gene in intergenic region; 5' UTR: processed from mRNA 5' end; 3' UTR: processed from mRNA 3' end; antisense: antisense to an annotated gene; IGR/as: free-standing sRNA gene in intergenic region extending into an annotated gene; 3' UTR op: free-standing sRNA gene overlapping the 3' end of an annotated gene). (B) Total RNA samples of WT and Δ*hfq* cells were collected at indicated time-points (OD_{600} of 0.25 to 2 and 3h after cells reached OD_{600} of 2) during growth in LB and subjected to Northern blot analysis. KpnR_128 is expressed from its own promoter internal to another transcriptional unit positioned upstream. Both transcripts share the same termination site and the ~300 nt transcript (#) is thus detected by the Kpn_R128 probe. 5S rRNA served as loading control.

Supplementary Figure S4

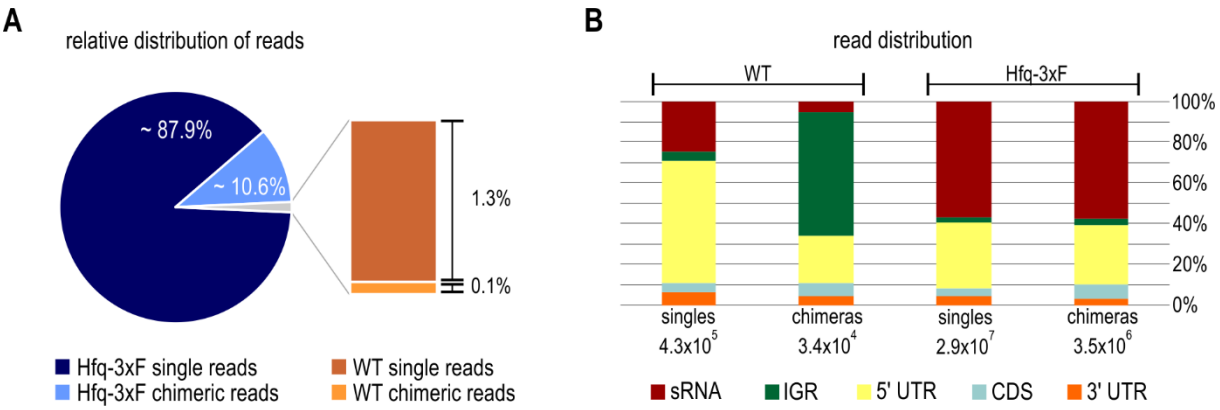

Relative read distribution in the RIL-seq experiment. (A) Distribution of filtered single and chimeric reads in samples recovered from the RIL-seq experiment in *K. pneumoniae* wild-type (WT) or *hfq::3xFLAG* (Hfq-3xF) cells. (B) Distribution of different RNA classes in single and chimeric reads in samples recovered from the RIL-seq experiment in *K. pneumoniae* wild-type or *hfq::3xFLAG* cells.

Supplementary Figure S5

A

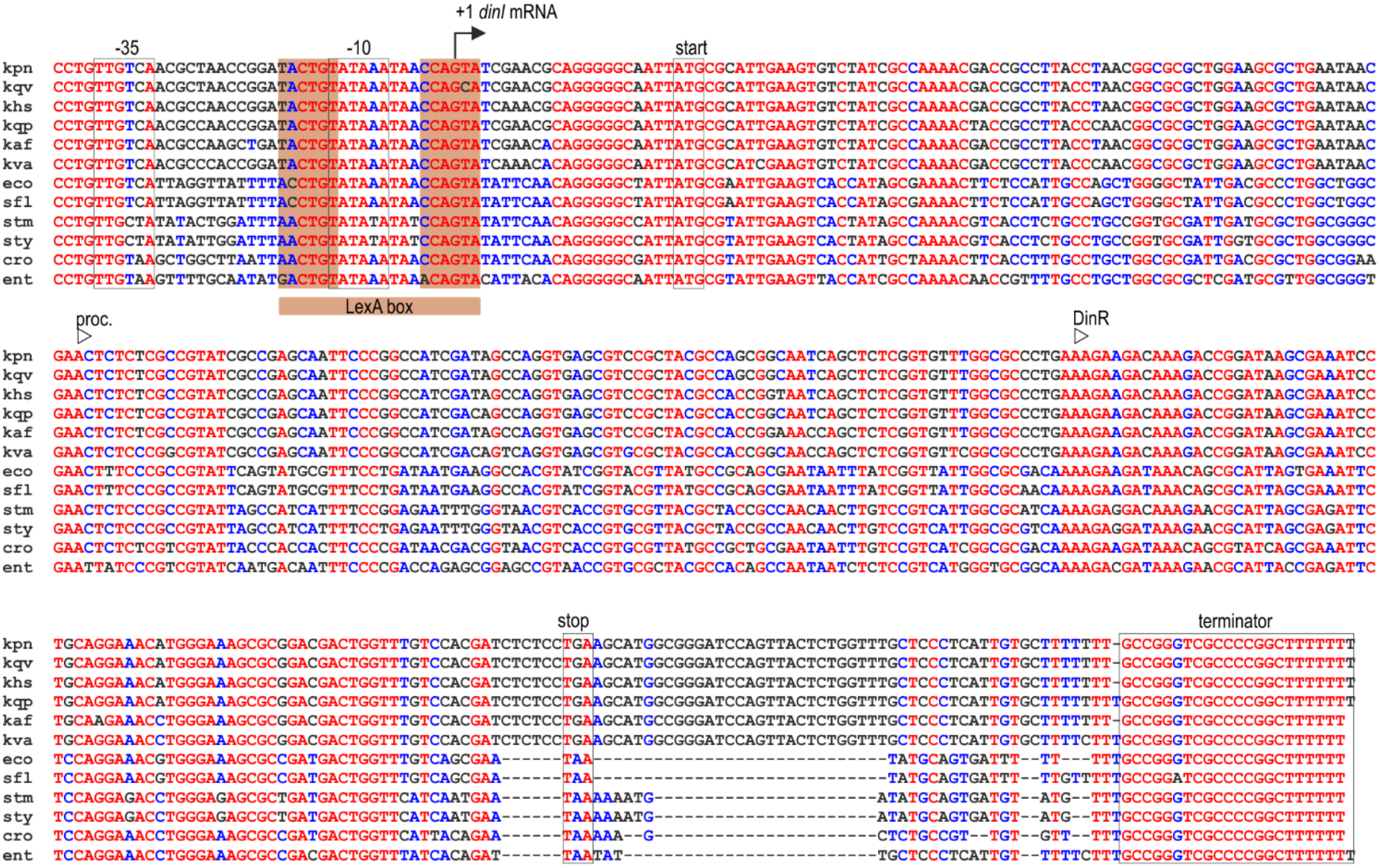

B

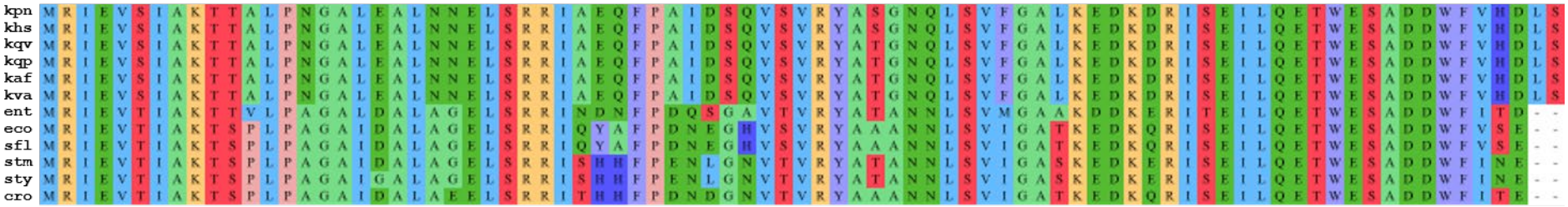

Conservation of *dinI* in enterobacteria. (A) Multiple alignment of the *dinI* gene of different enterobacterial species (kpn: *Klebsiella pneumoniae* MGH 78578; kqv: *Klebsiella quasivariicola* 08A119; khs: *Klebsiella pneumoniae subsp. pneumoniae* HS11286; kqp: *Klebsiella quasipneumoniae* KqPF26; kaf: *Klebsiella africana* 200023; kva: *Klebsiella variicola* LEMB11; eco: *Escherichia coli* MG1655; sfl: *Shigella flexneri* 301; stm: *Salmonella* Typhimurium LT2; sty: *Salmonella typhi* CT18; cro: *Citrobacter rodentium* ICC168; ent: *Enterobacter sp.* 638) was calculated using the MultAlin tool (2). Nucleotides are colored regarding their degree of conservation (red: high conservation; blue: partial conservation; black: little or no conservation). The -10 and -35 elements of the *dinI* promoter, as well as the start and stop codons and the Rho-independent terminator are boxed, the transcriptional start site (as determined for *K. pneumoniae*; compare Fig. S6) is indicated by an arrow. The 5’ ends of the two most abundant processing intermediates (proc. and DinR) from *dinI* mRNA in *K. pneumoniae* MGH 78578 are indicated by open triangles. The LexA box of *dinI* (as determined for *E. coli* in (3, 4)) is highlighted in orange. (B) Multiple alignment of the DinI protein of different enterobacterial species (as in (A)) was calculated using the MAFFT tool (5).

Supplementary Figure S6

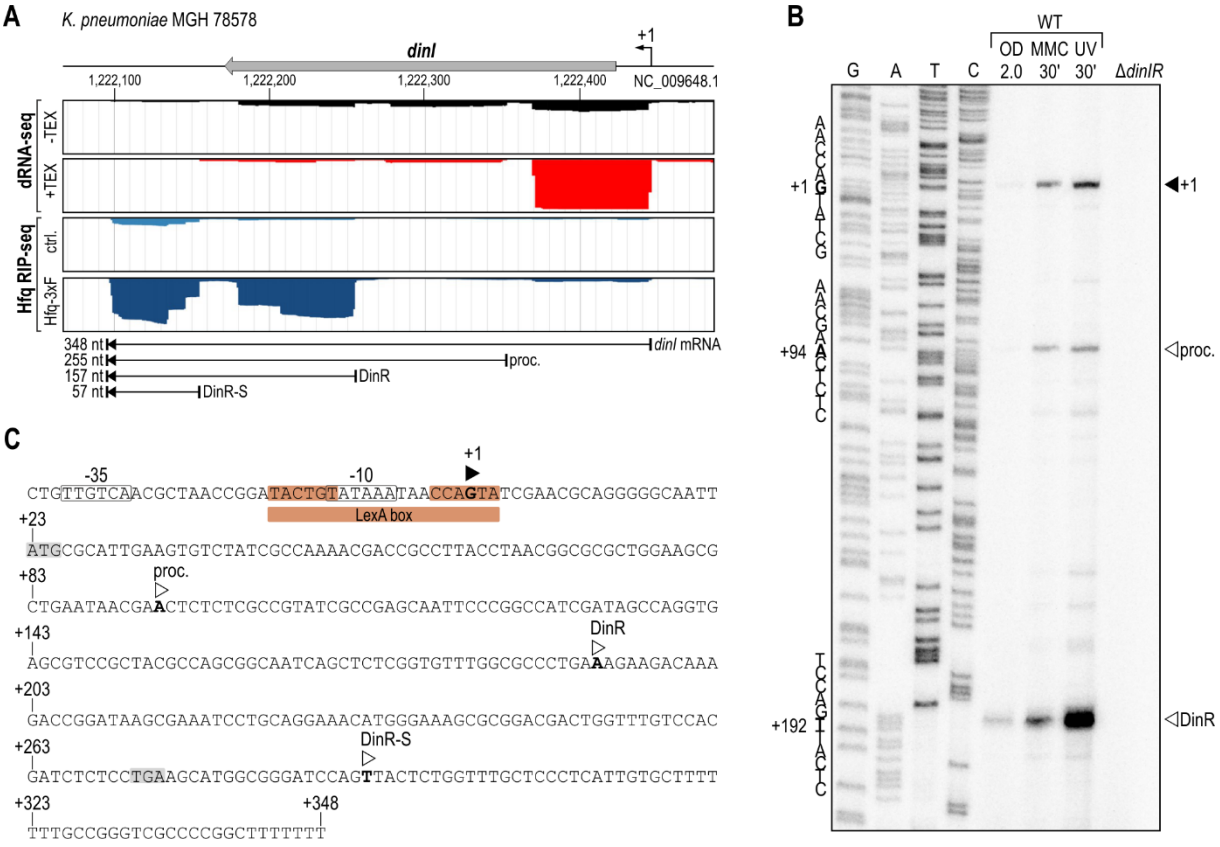

Determination of the 5' ends of *dinI* mRNA and its major processing products. (A) Read-mappings of dRNA-seq (-TEX: black traces; +TEX: red traces) and Hfq RIP-seq (control: light blue traces; Hfq-3xFLAG: dark blue traces) to the *dinI* locus. The y-axes in individual experiments were set to the same scale. The positions on the *K. pneumoniae MGH 78578* genome are indicated above the sequencing traces, and the *dinI* CDS is indicated by a grey arrow. The TSS of *dinI* was determined by analysis of the dRNA-seq dataset, and is marked by a black arrow. Stable processing products were identified from dRNA-seq and Hfq RIP-seq and sizes are below the panels. (B) Primer extension analysis of *dinI* mRNA (using a gene-specific primer). RNA was extracted from wild-type cells at OD_{600} of 2.0, and 30 min after DNA damage was induced through mitomycin C (MMC) or ultraviolet light (UV). RNA purified from *dinIR* mutant cells served as a control. The 5' ends of *dinI* mRNA (black arrowhead) and its processing products (proc. and DinR; open arrowheads; DinR-S is too close to the 3' end to be resolved in this experiment) were mapped using a sequencing ladder, and correspond to the sites determined by dRNA-seq. (C) Sequence at the *dinI* locus of *K. pneumoniae MGH 78578*. The -35 and -10 elements of the *dinI* promoter are boxed, the LexA box is high-lighted in orange. The 5' ends of *dinI* mRNA (black arrowhead) and its processing products (proc., DinR, DinR-S; open arrowheads) are indicated. Numbering refers to the TSS as position +1.

Supplementary Figure S7

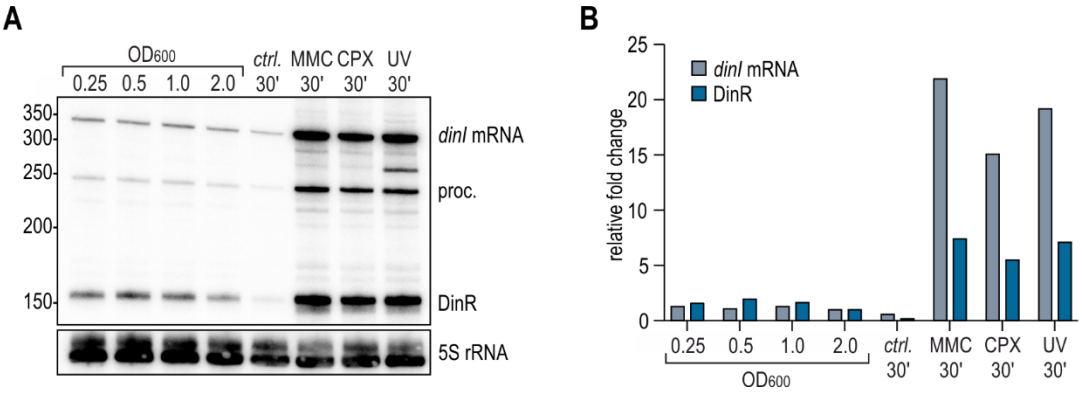

Expression of *dinI* mRNA and DinR sRNA in *K. pneumoniae*. (A) RNA samples were collected at different time-points over growth (OD_{600} from 0.25 to 2.0), and 30 min after cells had reached an OD_{600} of 2.0 in the absence (*ctrl.*) or presence of DNA damage induced through mitomycin C (MMC), ciprofloxacin (CPX) or ultraviolet light (UV). Expression of *dinI* mRNA and DinR was assessed by Northern blot analysis; 5S rRNA served as loading control. (B) Quantification of *dinI* mRNA and DinR sRNA signals relative to the expression at OD_{600} of 2.0.

Supplementary Figure S8

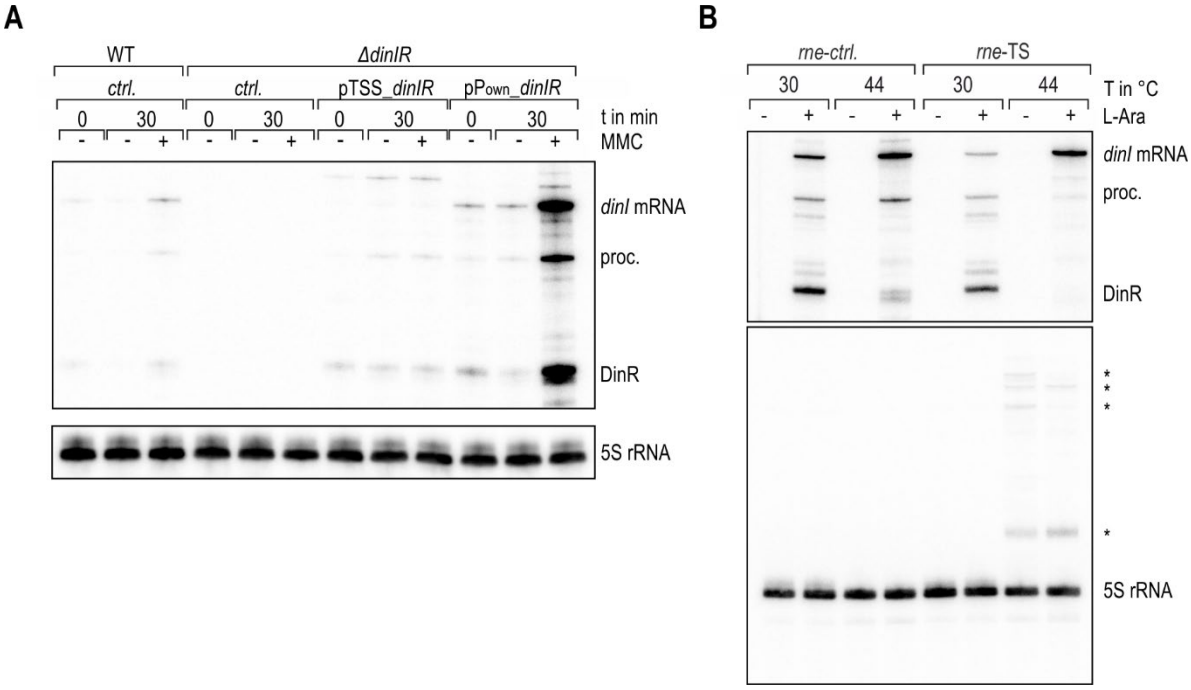

DinR is processed from the *dinI* mRNA. (A) *K. pneumoniae* WT or Δ*dinIR* cells carrying either an empty control vector (pBAD$_{KP}$-*ctrl.*) or plasmids harbouring different variants of the *dinI* gene (either starting from the TSS [pTSS_*dinIR*] or 50 bp upstream of the TSS [pP$_{own}$_*dinIR*]) were grown to OD$_{600}$ of 2.0, when DNA damage was induced by the addition of MMC. DinR and *dinI* mRNA levels were determined by Northern blot analysis of RNA samples collected at the indicated time-points. 5S ribosomal RNA served as a loading control. (B) *Salmonella* Typhimurium expressing a temperature-sensitive RNase E variant *(rne*-TS) or an isogenic control strain (*rne-ctrl.*) were transformed with pBAD$_{EC}$-*dinIR* and grown to OD$_{600}$ of 0.25 at the non-permissive temperature of 30 °C. Cultures were split and cultivation was continued for 45 min at 30 °C or at 44 °C to inactivate RNase E. RNA samples were collected prior to (-) and 15 min after (+) induction of *dinIR* expression with arabinose. Expression of *dinI* mRNA and DinR were determined by Northern blot analysis. 5S ribosomal RNA served as a loading control, and accumulating precursors of 5S rRNA are indicated by asterisks.

Supplementary Figure S9

A

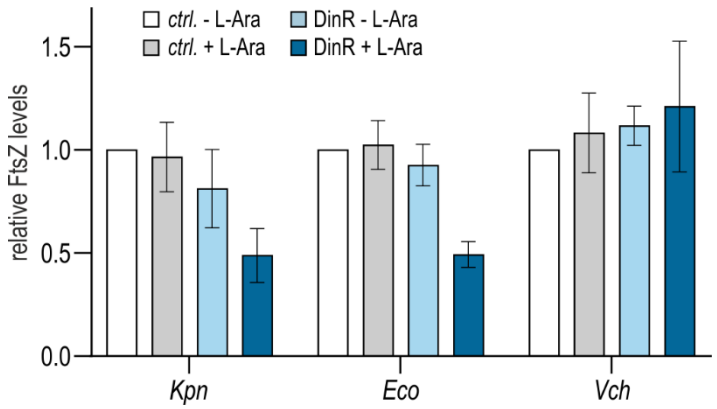

B

```
kpn AAAAGAGTTTTAATTTTTTAAGAGAACGCAGACAATTAGCGTTCTCAG-GCGACAGGCACAAGACGGAGAGAAACTATG
cko AAAAGAGTTTTAATTTTT-ATGAGACCGGCGACTATTAACGGTCTCAG-GCGACAGGCACAAAACGGAGAGAAACTATG
eco AAAAGAGTTTTAATTTTT-ATGAGGCCGACGATGATTA-CGGCCTCAG-GCGACAGGCACAAATCGGAGAGAAACTATG
sfl AAAAGAGTTTTAATTTTT-ATGAGGCCGACGATGATTA-CGGACTCAG-GCGACAGGCACAAATCGGAGAGAAACTATG
stm AAAAGAGTTTTAATTTTT-ATGAGGCCGCCAGATATTA-CGGCCTCAG-GCGACAGGCACATGACGGAGAGAGATTATG
vch AAAAGAGTTTTAA------------------------------C-CTGAGAGACAGGAAA--AACGGAGATAACACATG
```

Regulation of *ftsZ* expression and conservation of the 5' UTR. (A) Quantification of FtsZ protein levels. FtsZ expression was determined by Western blot analysis using a FtsZ-specific antiserum in total protein samples collected from *K. pneumoniae*, *E. coli* and *V. cholerae* carrying either an empty control vector (pBAD$_{KP}$-*ctrl.*, pBAD$_{EC}$-*ctrl.*, or pBAD$_{VC}$-*ctrl.*, respectively) or pBAD variants for the expression of DinR (pBAD$_{KP}$-DinR, pBAD$_{EC}$-DinR, or pBAD$_{VC}$-DinR, respectively). Bacteria were diluted from overnight cultures into fresh medium, and sRNA expression was induced by the addition of arabinose for 5 hours. FtsZ levels in the control sample (- L-Ara) was set to 1; error bars denote the standard deviation from five biological replicates. (B) Non-redundant alignment of the *ftsZ* 5' UTR of different bacterial species (kpn: *Klebsiella pneumoniae* MGH 78578; cko: *Citrobacter koseri* ATCC BAA-895; eco: *Escherichia coli* MG1655; sfl: *Shigella flexneri* 301; stm: *Salmonella* Typhimurium LT2; vch: *Vibrio cholerae* O1 El Tor N16961) was calculated using the Multalign tool (2). The stop codons of the upstream gene *ftsA* and the start codons of *ftsZ* are underlined, two transcriptional start sites (as determined by dRNA-seq in *K. pneumoniae*) are indicated by arrows. All nucleotides are colored with regard to their degree of conservation (red: high conservation; blue: partial conservation; black: little or no conservation).

Supplementary Figure S10

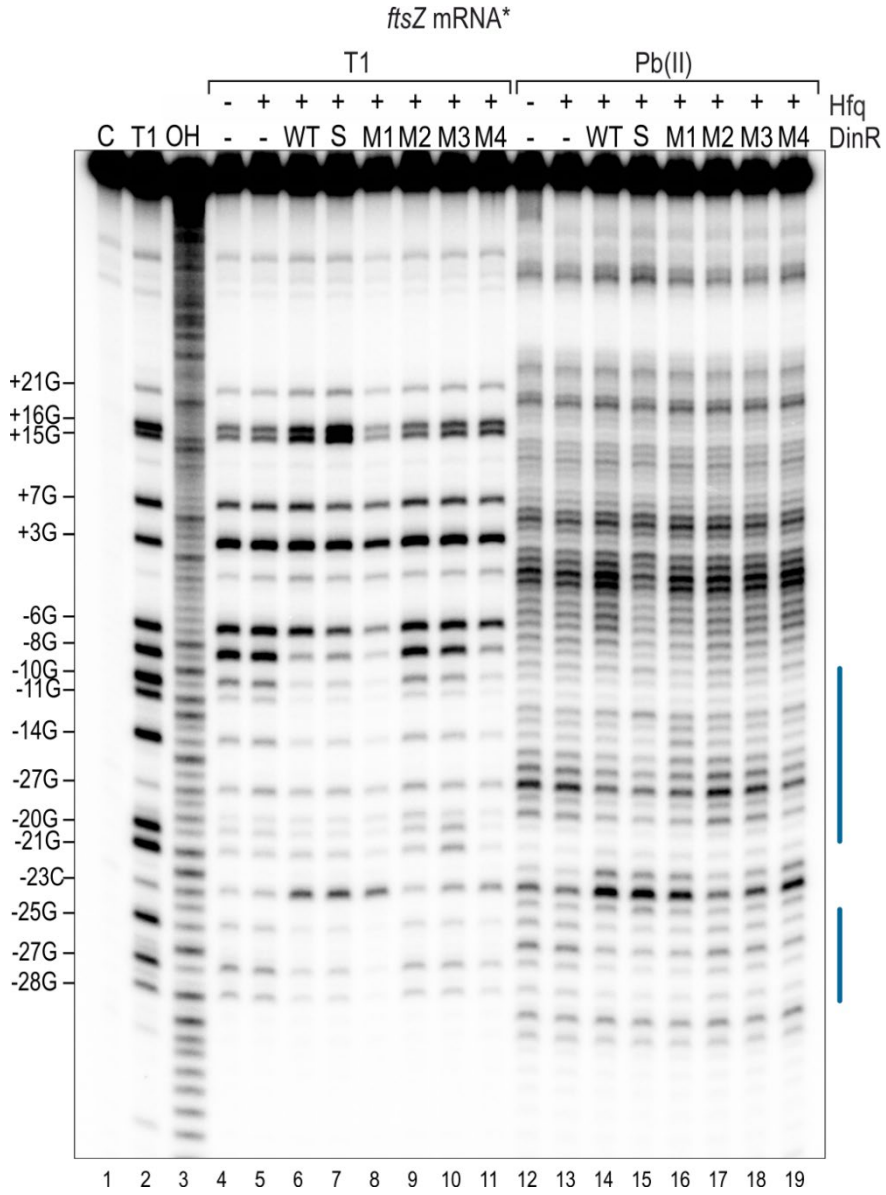

***In vitro* analysis of DinR base-pairing on *ftsZ* mRNA.** Structure probing of 5′ end-labelled *ftsZ* mRNA (TSS at –58 to +60 relative to the start codon; 0.4 pmol) with RNase T1 (lanes 4 to 11) and lead(II) acetate (lanes 12 to 19) in the absence or presence of 2 pmol (5x) Hfq protein and 4 pmol (10x) sRNAs DinR (WT), DinR-S (S), or DinR variants (M1-M4; compare 5(B)). RNase T1 and alkaline ladders of the *ftsZ* transcript were used to map the positions of individual nucleotides. The positions of G residues are indicated relative to the translational start site. Putative DinR binding sites are marked in blue.

Supplementary Figure S11

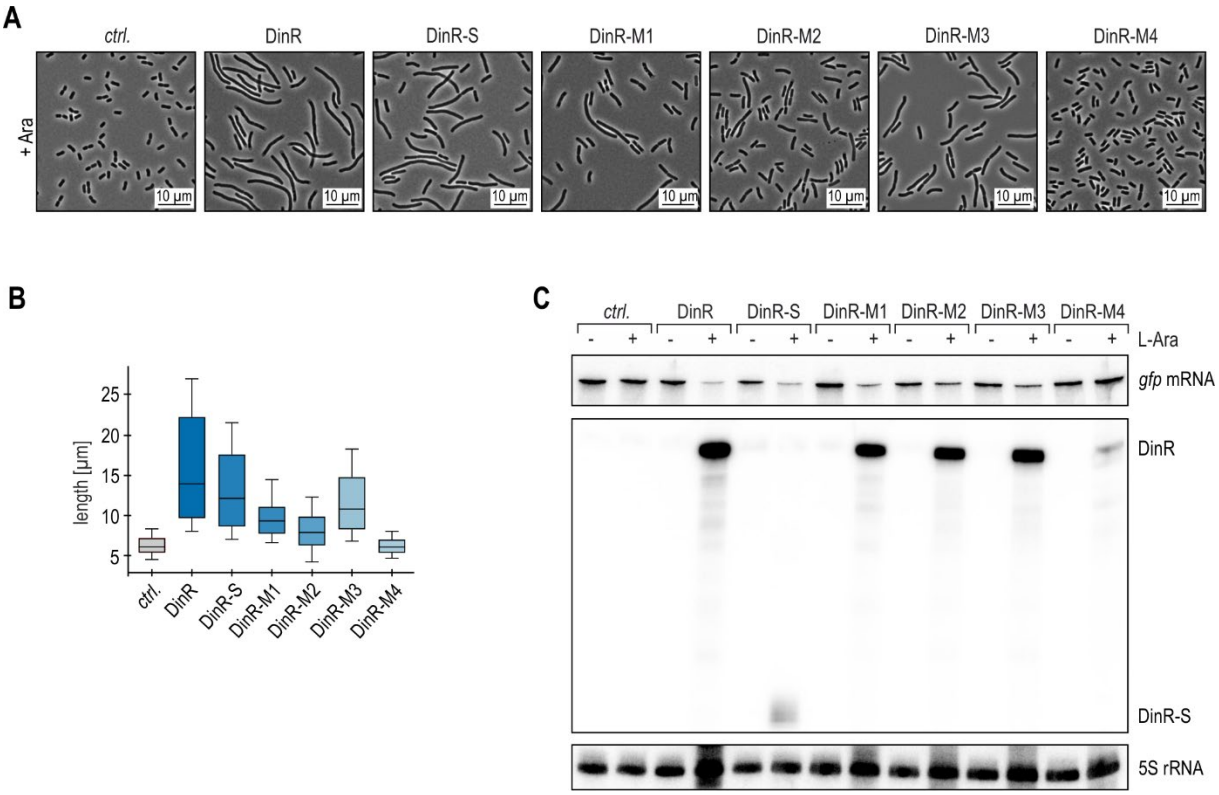

DinR overexpression causes cell filamentation. (A) *K. pneumoniae* carrying either an empty control vector ($pBAD_{KP}$-*ctrl.*) or $pBAD_{KP}$ variants for the expression of DinR, DinR-S, DinR-M1, DinR-M2, DinR-M3 or DinR-M4 were diluted from overnight cultures into fresh medium, and sRNA expression was induced by the addition of arabinose. Cell morphology was assessed by phase contrast microscopy after 5 hours. (B) Analysis of cell lengths in samples described in (A). The center line indicates the median, boxes represent the 25th and 75th percentiles, and lower and upper whiskers represent the 10th and 90th percentiles, respectively. (C) *E. coli* carrying the post-transcriptional *ftsZ::gfp* reporter and either $pBAD_{EC}$-*ctrl.* or $pBAD_{EC}$ variants for the expression of DinR, DinR-S, DinR-M1, DinR-M2, DinR-M3 or DinR-M4 were grown to OD_{600} of 0.5. Total RNA samples were prepared from cells collected prior to (-) or 10 min after the addition of arabinose (+). DinR and *ftsZ::gfp* mRNA levels were determined by Northern blot analysis; 5S ribosomal RNA served as a loading control.

Supplementary Figure S12

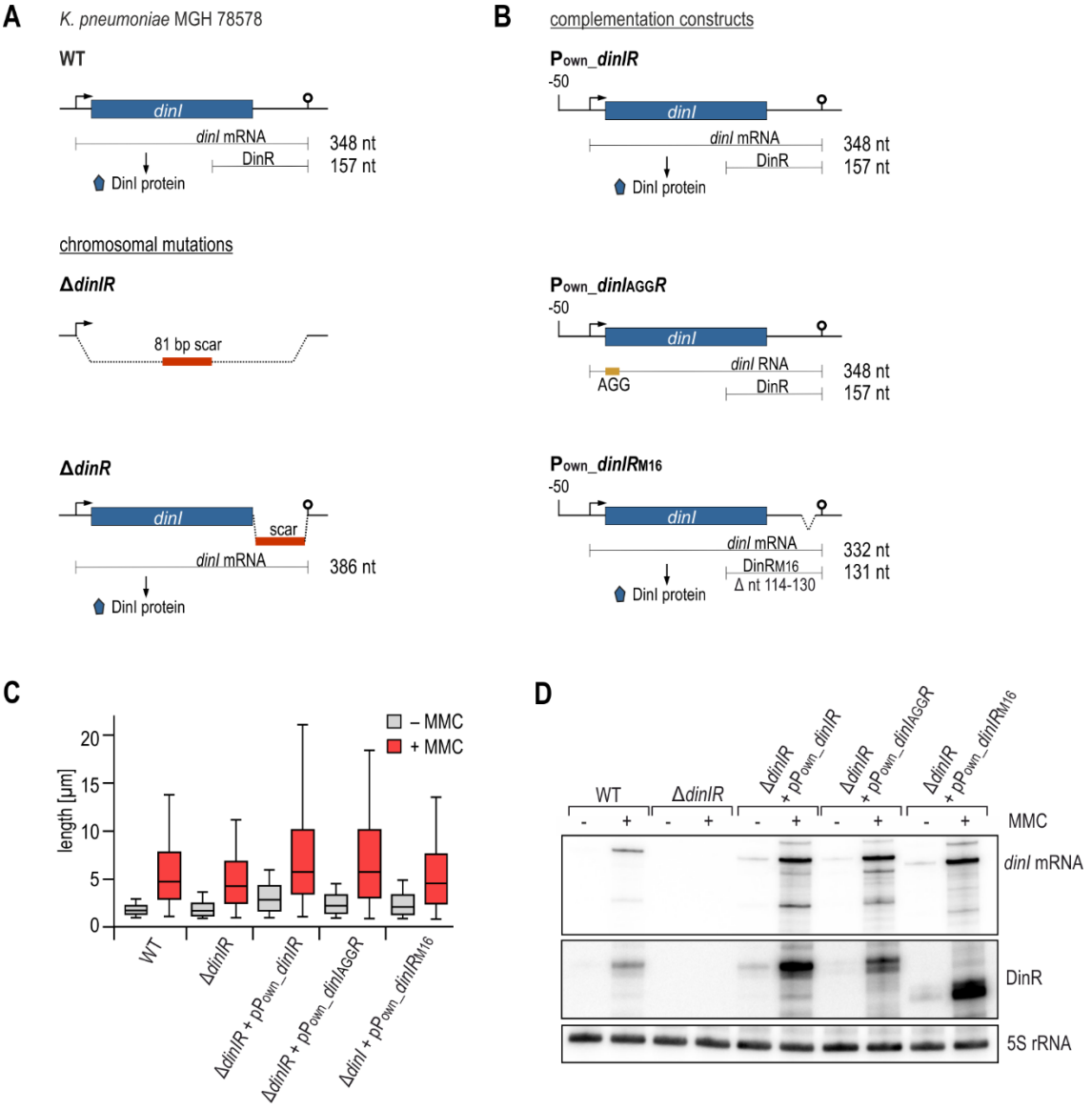

Complementation of the *dinIR* mutant. (A) Schematic of the *dinIR* locus of *K. pneumoniae* in wild-type and mutant cells. In the chromosomal mutant Δ*dinIR* deletion, a 81 bp scar replaces the sequence from the TSS to the end of the 3' UTR. In the chromosomal mutant Δ*dinR*, a 81 bp scar replaces the sequence from the stop codon to the beginning of the terminator hairpin (nt 84 to 126 of the sRNA). The size of the *dinI* mRNA increases to 386 nt. (B) Schematic of complementation constructs of *dinIR*. Plasmid pP$_{own}$_*dinIR* expresses *dinIR* under control of its own promoter; DinI protein is produced. Plasmid pP$_{own}$_*dinI*$_{AGG}$*R* expresses *dinIR* under control of its own promoter; the stop codon of *dinI* is changed from ATG to AGG; DinI protein is not produced. Plasmid pP$_{own}$_*dinIR*$_{M16}$ expresses *dinIR* under control of its own promoter; nt 114 to 130 of DinR have been deleted; DinI protein is produced. (C) *K. pneumoniae* wild-type cells or *dinIR* mutant cells carrying complementation plasmids (as described in (B)) were diluted from overnight cultures into fresh medium, split and either treated with MMC (1 µg/mL) to induce DNA damage or left untreated. Cell morphology was assessed by phase contrast microscopy after 5 hours and quantified. The center line indicates the median, boxes represent the 25th and 75th percentiles, and lower and upper whiskers represent the 10th and 90th percentiles, respectively. (D) RNA samples prepared from cells treated as described in (C) were analyzed on Northern blot; 5S ribosomal RNA served as a loading control.

SUPPORTING METHODOLOGY

Construction of Bacterial Strains

Klebsiella pneumoniae subsp. pneumoniae MGH 78578, *E. coli* Top10 and *V. cholerae* C6706 are referred to as wild-type strains in this study.

Plasmids were introduced in *K. pneumoniae* and *E. coli* by electrotransformation, and into *V. cholerae* by conjugation via the *E. coli* S17 helper strain using standard protocols. To construct chromosomal mutations, we followed a published procedure based on the widely-used *E. coli* one-step inactivation method based on the λ-Red recombinase system (6). Briefly, wild-type cells carrying pACBSR-Hyg (encoding the λ-Red genes under control of the *araBAD* promoter) were transformed with PCR products (obtained by overlap extension PCR) containing the *aac(3)IV* gene (conferring apramycin resistance) flanked by FRT recombination sites and ~500 bp of sequences homologous to the genomic integration sites. For fragments carrying the *aac(3)IV* marker gene, pIJ773 (KFO-1407/KFO-1376) or pER15 (KFO-1375/KFO-1376) were amplified and combined with individual flanking regions (Δ*hfq*: KFO-1252/KFO-1408 and KFO-1255/KFO-1378; *hfq*-3xFLAG: KFO-1252/KFO-1377 and KFO-1255/KFO-1378; Δ*sulA*: KFO-1798/KFO-1800 and KFO-1799/KFO-1801; Δ*dinI*: KFO-1792/KFO-1821 and KFO-1905/KFO-1793; Δ*dinR*: KFO-1792/KFO-2001 and KFO-2000/KFO-1793). Transformants were recovered in the presence of apramycin, and desired mutations were confirmed by colony PCR and sequencing. The temperature-sensitive pACBSR-hyg was lost during growth in LB at 37 °C. To eliminate the *aac(3)IV* cassette, the resulting strain was transformed with pFLP-hyg, and expression of the FLP recombinase was induced with arabinose. Recombination at the FRT site and correct excision of the cassette was confirmed by colony PCR and sequencing, and the helper plasmid was removed by passaging cells at 37 °C. Multiple mutations were introduced by sequentially performing the genomic modifications described above.

Unexpectedly, introduction of the pACBSR-Hyg helper plasmid resulted in selective loss of accessory plasmids pKPN4 and pKPN6, respectively, from a subset of transformed wild-type *K. pneumoniae* MGH 78578, a phenotype that had not been reported in the original protocol. We thus verified that neither loss of the two plasmids nor addition of the epitope to the RNA-binding protein expressed from its native promoter in MGH 78578 impaired bacterial growth under standard conditions when compared to WT cells (Fig S2B). In addition, we performed phenotypic characterization of our results throughout the manuscript using an isogenic WT strain, in which pKPN4 and pKPN6 had been likewise removed.

Bacterial growth conditions

K. pneumoniae, Escherichia coli and *V. cholerae* strains were grown aerobically at 37 °C in LB broth or on LB agar. Where appropriate, media were supplemented with kanamycin (50 μg/mL), chloramphenicol (20 μg/mL), ampicillin (100 μg/mL), hygromycin (100 μg/mL), or apramycin (50 μg/mL). Expression from the araBAD promoter was induced with L-arabinose (final concentration: 0.2%). Unless stated otherwise, DNA damage was triggered in *K. pneumoniae* by adding mitomycin C (MMC; 0.5 μg/mL) or ciprofloxacin (CPX; 4 μg/mL) to the culture, or by irradiation with UV light (λ=254 nm; 10 mJ/cm^2).

Plasmid construction

All plasmids and oligonucleotides used in this study are listed in Tables S4 and S5.

A template plasmid (pER15) for the chromosomal integration of the 3xFLAG epitope tag was constructed via PCR amplification of pIJ773 (KFO-1250/KFO-1251), and self-ligation was carried out as in (7).

The translational GFP reporter fusion of *ftsZ* (pFS7) was constructed via Gibson assembly (GA; NEB #E2611L) as recommended by the manufacturer using a PCR product amplified

from *K. pneumoniae* genomic DNA (KFO-1713/KFO-1714) and the linearized pXG10 vector (KPO-1702/KPO-1703). For the construction of the *ftsZ(M3)::gfp* variant (pER44), plasmid pFS07 was used as a template in PCR amplification with primer set KFO-1851/KFO-1852, and the obtained fragment was self-ligated.
For plasmids expressing DinR from the arabinose-inducible pBAD plasmid, inserts amplified from *K. pneumoniae* genomic DNA were cloned into linearized vectors via GA. For expression in *E. coli*, backbone pKP8-35 was amplified via KPO-0196/KPO-0411 and combined with an insert amplified with KFO-1718/KFO-1716. For expression in *V. cholerae*, backbone pBAD1K was amplified via KPO-0196/KPO-1397 and combined with an insert amplified with KFO-1715/KFO-2140. For expression in *K. pneumoniae*, an apramycin resistance cassette (amplified from pIJ773 with KFO-1830/KFO-1831) was introduced into pKP8-35 (linearized with KFO-1832/KFO-1833), and the obtained plasmid (pER41) was amplified via KPO-0196/KPO-0411 and combined with an insert amplified with KFO-1718/KFO-1716 by GA.
For plasmids expressing variants of DinR, pFS1 or pER41 served as a template for PCR amplification with primer pairs KFO-1992/KFO-1993 (pER66 and pER90); KFO-1892/KFO-1893 (pFS51 and pER85); KFO-1849/KFO-1850 (pER43 and pER84); KFO-1990/KFO-1991 (pER65 and pER89), and obtained fragments were self-ligated.
To verify transcriptional control of DinR expression, two variants of *dinI* lacking (KFO-2028/KFO-1716; pER82) or including the annotated promoter (KFO-2029/KFO-1716; pER83) were inserted via GA into linearized pER41 lacking the *araBAD* promoter (amplified by KFO-2027/KPO-0411). Plasmid pER83 served as template for PCR amplification with primer pairs KFO-2719/KFO-2720 to obtain pER156 and with KFO-2721/KFO-2723 to obtain pER158.

T7 transcription and 5' end-labelling of RNA

RNA was *in vitro* synthesized and 5' end-labelled as described before (8, 9). In short, DNA templates carrying the T7 promotor were amplified by PCR using the oligonucleotides listed in Table S5. *In vitro* transcription of RNA from template DNA was performed using the AmpliScribe T7-Flash transcription kit (Epicentre). RNA was dephosphorylated using calf-intestinal alkaline phosphatase (NEB), subsequently extracted with P:C:I (phenol/chloroform/isoamyl alcohol; 25:24:1) and ethanol precipitated. 5' end labelling was achieved by incubation of dephosphorylated RNA with [32P]- γATP and polynucleotide kinase (NEB) for 1 h at 37 °C. Unincorporated nucleotides were removed using Amersham MicroSpin G-50 columns (Cytiva). Labelled RNA was then purified on a denaturing 6 % PAA / 7 M Urea gel, eluted with RNA elution buffer (0.1 M sodium acetate, 0.1 % SDS, 10 mM EDTA) at 4 °C overnight and recovered by P:C:I extraction.

Riboprobes

The riboprobes to detect DinR, *dinI* and *sulA* mRNAs were synthesized by T7-mediated *in vitro* transcription of ~200 ng of template DNA (amplified on *Klebsiella* gDNA with KFO-1762/KFO-1763; KFO-2554/KFO/2555; KFO-2288/KFO-2260) in the presence of [^{32}P]-α-UTP with the MAXIscript T7 transcription kit (Invitrogen). Unincorporated nucleotides were removed using MicroSpin G-50 columns (Cytiva).

Primer extension analysis

For primer extension, 5 µg of RNA were denaturated in the presence of 1 pmol 5′ end-labelled primer (KFO-1745) at 70°C for 2 min and adjacently chilled on ice for 5 min. Next, the samples were mixed with the reaction mix (1X first strand buffer, 5 mM DTT, 0.5 mM each dATP, dGTP, dCTP and dTTP) at 42°C, and SuperScript III (100 U; Invitrogen) was added. cDNA synthesis was performed at 50°C for 60 min, followed by incubation at 70°C for 15 min to inactivate the enzyme. Samples were treated with RNase H (2.5 U) for 15 min at 37°C and the reaction was

stopped by the addition of GLII loading buffer. Samples was separated by electrophoresis on a 6% sequencing gel together with a template-specific ladder (prepared using the SequiTherm EXCELII DNA Sequencing Kit).

dRNA sequencing

In brief, RNA samples were fragmented using ultrasound, followed by treatment with polynucleotide kinase (PNK). For the depletion of processed transcripts and the control reaction, equal amounts of RNA were incubated with or without terminator 5′-phosphate-dependent exonuclease (TEX; Lucigen). RNA samples were poly(A)-tailed using poly(A) polymerase and 5′-triphosphates were removed by applying tobacco acid pyrophosphatase (TAP). An RNA adapter was ligated to the 5’ end of the RNA prior to cDNA synthesis using an oligo(dT) primer and M-MLV-RNase H- reverse transcriptase. Upon amplification of the cDNA with a high-fidelity polymerase and gel fractionation, the resulting libraries were pooled and sequenced on an Illumina NextSeq 500 system with 1x75 bp read length.

Sequencing reads from the dRNA-seq experiment were processed and analysed according to (10) with minor modifications. Briefly, for every replicate in both conditions, the coverage and based on it, the difference between neighboring nucleotides was computed. Local maxima in the differences were called as TSS if the difference between maximum and minimum coverage in a 7 nt window around the TSS was above 3 TPM, and the ratio between the maximum and the minimum was above 1.3. The set of putative TSS was manually curated and the resulting predictions were used to annotate genes with a 5’ UTR within a window of 250 nt upstream of an annotated gene. The most distant TSS was then used to define the 5’ UTR of the corresponding gene. 3’ UTRs were annotated by extending an area downstream of a gene, up to 150 nt in length unless the next annotation was closer than that window. Custom scripts are available from GitHub (https://github.com/maltesie/KpnInteractomePaper; DOI: 10.5281/zenodo.8409716).

Hfq RIP-seq analysis

Demultiplexed raw reads were imported into the CLC Genomics Workbench (Qiagen) and subjected to quality control and adaptor trimming. The trimmed reads were mapped to the *Klebsiella pneumoniae subsp. pneumoniae* MGH 78578 reference genome (NCBI accession numbers NC_009648.1, NC_009649.1, NC_009651.1, and NC_009653.1) with standard parameter settings. Annotations of sRNAs were added manually. Fold enrichment in samples expressing Hfq-3xFLAG over the untagged control samples was calculated using the CLC “Differential Expression for RNA-Seq” tool.

RIL-seq analysis

Briefly, cells corresponding to 40 OD_{600} units were subjected to UV crosslinking of proteins and RNA followed by cell lysis and co-immunoprecipitation using a monoclonal anti-FLAG antibody (Sigma; #F1804). Recovered RNA was trimmed by RNase A/T1 treatment, and proximal RNAs were ligated. Upon proteinase K treatment, RNA was extracted, fragmented and DNase digested. A previously published protocol (11) was adapted for the strain-specific depletion of ribosomal RNA. Co-immunoprecipitated RNA samples were mixed with an oligonucleotide mix (final concentrations: 5.8 nM for 16S and 23S oligos; 11.6 nM for 5S oligos) in the presence of 1x SSC and 1 mM EDTA. The mixture was denatured, cooled down and incubated with streptavidin beads (ThermoFisher; #65001) in 0.5x SSC at room temperature and 50°C for 5 min each, respectively. Depleted RNA in the supernatant was purified using AMPure XP beads (Beckman-Coulter; #A63881) and subjected to cDNA library preparation. Upon PCR amplification, libraries were sequenced in paired-end mode on an Illumina NextSeq 1000 with 150 bp read-length.

The sequence file was demultiplexed using the split_libs command from RNASeqTools (DOI: 10.5281/zenodo.8388882) and the resulting files were analyzed with ChimericFragments (DOI: 10.5281/zenodo.8376810) used with the default parameters set except for the following: min_seed_length=15, autocomplete_utrs=false, bp_shift_weight=0.0, max_bp_fdr=0.35 and min_reads=5 as described in (12).

Annotation of sRNAs

Complementation of sRNA annotation was based on several criteria. Conserved enterobacterial sRNAs were identified by comparison with published datasets (13-16). Candidate sRNAs in IGRs were selected if a clear TSS, a length ranging from 50 to 350 nts, and a termination site were identified; sequences were scanned for putative ORFs (≥ 20 aa).
5' UTR-derived sRNAs were annotated based on the detection of a processing site or a sharp drop in coverage upstream of the translational start site of the associated mRNA. 3' UTR-derived sRNAs were selected based on the presence of a processing site or a TSS within the 3' end of the associated mRNA and a shared termination site.

Identification of LexA motifs

To identify previously unknown sRNAs contributing to the regulation of the SOS response we examined the Hfq RIP-seq dataset for potentially LexA-controlled transcripts, exploiting our accurate annotation of TSSs by dRNA-seq. We used MEME (17) to compute a LexA position weight matrix based on the sequences of 21 known SOS boxes of *E. coli* (3), and then searched for the obtained motif (WACTGTATATWHAHMCAGTA) within *K. pneumoniae* transcription initiation sites (-70 to +30 relative to the TSS). We identified putative LexA binding sites preceding 71 transcription units (see Table S2).

Chromatin immunoprecipitation (ChIP)

ChIP was performed following the previously published procedures (4, 10) with minor modifications. In brief, *K. pneumoniae* MGH 78578 wild-type cells were grown in two biological replicates in LB medium to a final OD_{600} of 2.0. The culture was split, and incubation was continued for an additional 30 min in the presence or absence of MMC (1 µg/mL).
Formaldehyde was added at a final concentration of 1% to cross-link DNA and proteins, and the reaction was quenched after 20' by the addition of glycine (0.5 M). Cells were washed in 1x TBS, and lysed in lysis buffer (50 mM Hepes-KOH pH=7.0, 150 mM NaCl, 1 mM EDTA, 1% Triton X-100, 0.1% sodium deoxycholate, 0.1% SDS) containing 4 mg/ml lysozyme. DNA was sheared to an average size of ~200 bp using a BioRuptor (5x 30 s pulses). Insoluble material was removed by centrifugation, and a sample of the supernatant was stored as input control. The samples were mixed with protein A magnetic beads (Thermo Fisher #10001D), split and either incubated with anti-LexA antibody (Sigma #06-719; +AB) or no antibody (-AB) at 4°C overnight. Samples were washed twice in lysis buffer, once in modified lysis buffer (500 mM NaCl), once in ChIP wash buffer (10 mM Tris-HCl pH=8.0, 250 mM LiCl, 1 mM EDTA, 0.5% Nonidet-P40, 0.5% sodium deoxycholate), and once in TE. Samples were eluted in elution buffer (50 mM Tris-HCl, 1 mM EDTA, 1% SDS) at 65°C, and cross-linking was reverted by boiling samples (including the input) for 10 min. DNA was purified by P:C:I extraction, and analyzed by quantitative PCR (qPCR) using the GoTaq qPCR Master Mix (Promega #A6002) on a CFX96 Real-Time PCR system (Bio-Rad), with *sgrR* CDS as a control.

Image analysis

The pipeline detects the bacteria and includes a background subtraction, noise removal and automated thresholding. To prevent clustering of cells in close vicinity, a second branch segments the halo around each object and subtracts those from the results of the cell

thresholding. To resolve overlaps and measure cell lengths, the segmented objects are transformed into a graph structure that contains information about the cell's medial axis and diameter. This representation allowed the usage of an algorithm to split overlapping clusters into individual objects by the removal of junction vertices and addition of alternative edges minimize the cell curvature. The length of each graph component and thus the bacterial cell is determined by a JIPipe-provided operation.

A detailed explanation of the workflow and its individual components, all results as well as the utilized software versions, is available through https://asbdata.hki-jena.de/RuhlandEtAl2023_PNAS.

Supplementary Table S1 – sRNAs in *K. pneumoniae* MGH 78578

Number	alternative name	reference genome	left end	right end	strand	classification	reference	enrichment RIP-seq MEP	enrichment RIP-seq ESP	pot. ORF ≥ 20 aa [(a)]
KpnR_001	tpke11	NC_009648.1	15539	15614	+	IGR	(15)	n.d.	n.d.	
KpnR_002	DapZ	NC_009648.1	41908	41977	+	3' UTR	(15)	7.3	6.0	
KpnR_003	SroA	NC_009648.1	79067	79132	-	5' UTR	(15)	0.5	0.3	
KpnR_004	SgrS	NC_009648.1	81037	81261	+	IGR	(15)	n.d.	n.d.	
KpnR_005	KPN_RS00380_5' (sRNA 1)	NC_009648.1	81244	81448	+	5' UTR	(14)	0.4	2.5	
KpnR_006	pdhR_3'	NC_009648.1	137318	137597	+	3' UTR	this study	0.6	3.2	
KpnR_007	tp2	NC_009648.1	137544	137673	-	IGR	(15)	1.8	7.9	
KpnR_008	rpsB_5'	NC_009648.1	215558	215695	+	5' UTR	(15)	0.3	0.2	
KpnR_009	rpsB_3'	NC_009648.1	216411	216509	+	3' UTR	this study	12.0	33.7	
KpnR_010	SraA	NC_009648.1	442430	442486	-	IGR	(15)	n.d.	0.8	
KpnR_011	4.5S_RNA	NC_009648.1	461884	462024	+	IGR	(15)	0.4	0.2	
KpnR_012	ChiX	NC_009648.1	510362	510442	+	IGR	(15)	27.5	15.4	
KpnR_013	KPN_RS02895_5' (sRNA 6)	NC_009648.1	597429	597620	+	IGR	(14)	38.9	56.9	
KpnR_014	SroC	NC_009648.1	769973	770129	-	IGR	(15)	12.7	10.3	
KpnR_015	KPN_RS03910_3915_IGR	NC_009648.1	817664	817879	-	IGR	this study	10.6	3.6	33 aa
KpnR_016	SdhX	NC_009648.1	827990	828076	+	3' UTR	(15)	12.5	20.7	
KpnR_017	KPN_RS04185_AS	NC_009648.1	865729	865826	+	as	this study	1.0	0.3	
KpnR_018	KPN_RS04690_4695_IGR1	NC_009648.1	975650	975775	-	IGR	this study	21.1	10.2	25 aa
KpnR_019	KPN_RS04690_4695_IGR2	NC_009648.1	976289	976417	-	IGR	this study	9.2	3.9	
KpnR_020	RybB	NC_009648.1	984425	984505	-	IGR	(15)	16.6	6.6	
KpnR_021	KPN_RS05160_5165_IGR	NC_009648.1	1089328	1089557	-	IGR	this study	9.1	12.4	39 aa
KpnR_022	KPN_RS05190_3'	NC_009648.1	1097112	1097453	+	3' UTR	this study	16.4	4.8	
KpnR_023	ompA_5'	NC_009648.1	1121359	1121526	-	5' UTR	this study	132.2	12.6	
KpnR_024	KPN_RS31110_KPN_RS31115_IGR	NC_009648.1	1178232	1178539	+	IGR/as	this study	11.2	10.4	33 aa
KpnR_025	phoH_5'	NC_009648.1	1198613	1198845	+	5' UTR	this study	0.8	1.5	
KpnR_026	RtT_RNA_1	NC_009648.1	1200277	1200414	-	IGR	(15)	0.5	2.3	
KpnR_027	RtT_RNA_2	NC_009648.1	1205516	1205645	-	IGR	(15)	3.6	n.d.	
KpnR_028	lpxP_3'	NC_009648.1	1217934	1218011	-	3' UTR	(15)	n.d.	n.d.	
KpnR_029	DinR	NC_009648.1	1222098	1222253	-	3' UTR	this study	4.6	5.3	
KpnR_030	SraB	NC_009648.1	1237475	1237592	+	IGR	(15)	3.3	0.3	
KpnR_031	KPN_RS05910_3'	NC_009648.1	1256448	1256635	+	3' UTR	this study	n.d.	36.1	
KpnR_032	potD_3'	NC_009648.1	1283992	1284057	-	3' UTR	this study	52.5	10.7	
KpnR_033	spy_5'	NC_009648.1	1378348	1378441	+	IGR	this study	19.8	13.1	

KpnR_035	spy3'	NC_009648.1	1379048	1379111	+	3' UTR	(15)	0.1	0.1	
KpnR_036	RyhB2	NC_009648.1	1404504	1404605	-	as	(15)	8.2	11.1	
KpnR_037	FnrS	NC_009648.1	1539850	1539972	+	IGR	(15)	26.2	7.4	
KpnR_038	KPN_RS07525_7530_IGR (sRNA 9)	NC_009648.1	1564287	1564584	+	IGR	(14)	26.7	9.3	
KpnR_039	KPN_RS32550_07555_IGR (sRNA 10)	NC_009648.1	1566904	1567072	+	IGR	(14)	0.8	9.2	
KpnR_040	KPN_RS28800_07710_IGR	NC_009648.1	1595047	1595119	-	IGR	this study	16.8	10.3	
KpnR_041	MicC	NC_009648.1	1603837	1603953	+	IGR	(15)	6.1	42.8	
KpnR_042	KPN_RS08035_8040_IGR (sRNA 12)	NC_009648.1	1668378	1668448	+	IGR	(14)	0.8	1.1	
KpnR_043	fumA_3'	NC_009648.1	1686189	1686371	+	3' UTR	this study	1.7	3.0	
KpnR_044	KPN_RS08415_8430_IGR1	NC_009648.1	1745512	1745772	+	IGR	this study	2.6	9.7	34 aa
KpnR_045	KPN_RS08415_8430_IGR2	NC_009648.1	1745946	1746213	+	IGR/as	this study	9.0	8.7	
KpnR_046	KPN_RS31250_31255_IGR	NC_009648.1	1772623	1772813	-	IGR/as	this study	1.6	5.0	34 aa
KpnR_047	MgrR	NC_009648.1	1792507	1792605	+	IGR	(15)	23.1	17.1	
KpnR_048	marA_AS	NC_009648.1	1805171	1805502	+	as	this study	23.8	9.2	
KpnR_049	KPN_RS09105_9110_IGR	NC_009648.1	1872673	1872791	+	IGR	this study	0.4	0.8	
KpnR_050	RydB	NC_009648.1	2117929	2118082	-	IGR	(15)	0.9	0.9	
KpnR_051	KPN_RS10415_3'	NC_009648.1	2131408	2131492	+	3' UTR op	this study	19.1	8.2	
KpnR_052	KPN_RS11045_30440_IGR (sRNA 14)	NC_009648.1	2246314	2246444	+	IGR	(14)	6.9	11.9	
KpnR_053	KPN_RS11175_AS	NC_009648.1	2271954	2272085	+	as	this study	11.4	8.3	
KpnR_054	KPN_RS11285_11290_IGR	NC_009648.1	2295887	2296029	+	IGR	this study	1.3	0.5	
KpnR_055	RprA	NC_009648.1	2367518	2367625	+	IGR	(15)	13.8	12.1	
KpnR_056	KPN_RS31415_11650_IGR	NC_009648.1	2370293	2370405	-	IGR	this study	24.5	13.3	
KpnR_057	OppX	NC_009648.1	2406354	2406535	-	5' UTR	(15)	8.3	5.1	
KpnR_058	dsbB_3'	NC_009648.1	2537931	2538143	+	3' UTR	this study	n.d.	12.6	
KpnR_059	SroD	NC_009648.1	2543260	2543341	-	3' UTR	(15)	1.6	0.0	
KpnR_060	KPN_RS12590_3'	NC_009648.1	2559201	2559318	+	3' UTR	this study	3.2	3.1	
KpnR_061	RydC	NC_009648.1	2580742	2580807	+	IGR	(15)	5.1	2.2	
KpnR_062	RyeA	NC_009648.1	2580911	2581210	+	IGR	(15)	1.5	1.0	
KpnR_063	SdsR	NC_009648.1	2580978	2581082	-	IGR	(15)	6.1	7.1	
KpnR_064	MicL	NC_009648.1	2609852	2610162	-	3' UTR op	(15)	5.8	n.d.	
KpnR_065	3'ETS-leuZ	NC_009648.1	2632966	2633029	-	3' UTR	(15)	9.9	12.5	
KpnR_066	DsrA	NC_009648.1	2645420	2645508	-	IGR	(15)	38.1	4.5	
KpnR_067	ompC_KPN_RS13105_IGR	NC_009648.1	2654265	2654491	+	IGR/as	this study	0.5	1.1	
KpnR_068	JUMPstart_RNA	NC_009648.1	2746038	2746142	-	IGR/as	(15)	1.1	1.0	
KpnR_069	KPN_RS1358_13585_IGR	NC_009648.1	2761160	2761273	+	IGR	this study	12.5	10.1	

KpnR_070	CyaR	NC_009648.1	2775703	2775790	+	IGR	(15)	28.9	23.6	
KpnR_071	MicF	NC_009648.1	2896241	2896333	+	IGR	(15)	18.3	9.4	
KpnR_072	nupC_3'	NC_009648.1	3017927	3018210	+	3' UTR	this study	3.0	3.1	
KpnR_073	STnc250	NC_009648.1	3075394	3075515	-	3' UTR	(15)	n.d.	n.d.	
KpnR_074	SroE	NC_009648.1	3122822	3122897	-	3' UTR	(15)	1.4	2.8	
KpnR_075	sseA_KPN_RS15310_IGR	NC_009648.1	3135762	3135917	-	IGR	this study	0.6	0.2	
KpnR_076	GlmY	NC_009648.1	3166842	3167027	-	IGR	(15)	0.3	0.5	
KpnR_077	RyfD	NC_009648.1	3207437	3207578	-	5' UTR	(15)	0.3	0.5	
KpnR_078	RaiZ	NC_009648.1	3210661	3210819	+	3' UTR	(15)	4.1	104.4	
KpnR_079	tmRNA	NC_009648.1	3231291	3231653	+	IGR	(15)	0.2	0.3	
KpnR_080	KPN_RS16030_3'	NC_009648.1	3290414	3290609	-	3' UTR op	this study	164.0	7.5	
KpnR_081	MicA	NC_009648.1	3318096	3318170	+	IGR	(15)	5.9	5.9	
KpnR_082	sok_AT	NC_009648.1	3394403	3394559	-	5' UTR	(15)	0.0	0.5	
KpnR_083	SokX	NC_009648.1	3394457	3394512	+	IGR	(15)	0.3	0.1	
KpnR_084	CsrB	NC_009648.1	3438471	3438838	-	IGR	(15)	0.5	0.8	
KpnR_085	GcvB	NC_009648.1	3469834	3470041	+	IGR	(15)	15.5	6.7	
KpnR_086	rppH_AS	NC_009648.1	3555242	3555333	+	as	this study	12.7	10.4	
KpnR_087	OmrA	NC_009648.1	3563070	3563157	-	IGR	(15)	12.4	7.1	
KpnR_088	OmrB	NC_009648.1	3563274	3563356	-	IGR	(15)	1.1	5.6	
KpnR_089	ompK26_3'	NC_009648.1	3587787	3587874	-	3' UTR	this study	7.8	4.1	
KpnR_090	6S_RNA	NC_009648.1	3665037	3665220	+	IGR	(15)	0.2	0.2	
KpnR_091	SibC	NC_009648.1	3665896	3666042	+	3' UTR	(15)	2.5	36.2	
KpnR_092	SroG	NC_009648.1	3778913	3779064	-	5' UTR	(15)	0.4	0.3	
KpnR_093	alx_5'	NC_009648.1	3878691	3878875	+	5' UTR	(15)	1.4	0.6	
KpnR_094	RnpB	NC_009648.1	3896359	3896741	-	IGR	(15)	0.3	0.4	
KpnR_095	SraG	NC_009648.1	3934702	3934873	+	IGR	(15)	0.6	0.0	
KpnR_096	ArcZ	NC_009648.1	3973082	3973203	+	IGR/as	(15)	14.2	8.1	
KpnR_097	RyhB	NC_009648.1	4161791	4161886	-	IGR	(15)	12.6	12.0	
KpnR_098	bscO_KPN_RS31745_IGR1 (sRNA 24)	NC_009648.1	4269680	4269841	+	IGR	(14)	3.1	4.0	
KpnR_099	bscO_KPN_RS31745_IGR2	NC_009648.1	4276216	4276497	+	IGR/as	this study	2.0	3.5	28 aa
KpnR_100	RtT_RNA_3	NC_009648.1	4277971	4278104	-	IGR	(15)	0.6	0.5	
KpnR_101	sok_AT	NC_009648.1	4299285	4299435	-	5' UTR	(15)	3.2	24.4	
KpnR_102	KPN_RS21245_21250_IGR (sRNA 25)	NC_009648.1	4314524	4314846	+	IGR/as	(14)	1.1	6.1	
KpnR_103	KPN_RS21430_waa_IGR	NC_009648.1	4355486	4355592	-	IGR/as	this study	1.2	1.5	
KpnR_104	IstR	NC_009648.1	4463773	4463903	-	IGR/as	(15)	0.9	0.4	

KpnR_105	KPN_RS22175_22180_IGR	NC_009648.1	4503473	4503564	+	IGR	this study	0.6	3.1	
KpnR_106	RbsZ	NC_009648.1	4553995	4554205	+	3' UTR op	(15)	n.d.	n.d.	
KpnR_107	Spot_42	NC_009648.1	4571507	4571625	+	IGR	(15)	30.0	17.0	
KpnR_108	CsrC	NC_009648.1	4572621	4572867	+	IGR	(15)	0.3	0.5	
KpnR_109	GlnZ	NC_009648.1	4577815	4577914	-	3' UTR	(15)	13.1	8.7	
KpnR_110	CpxQ	NC_009648.1	4622452	4622509	+	3' UTR	(15)	17.2	6.5	
KpnR_111	OxyS	NC_009648.1	4655076	4655194	-	IGR	(15)	18.7	17.0	
KpnR_112	GlmZ	NC_009648.1	4707421	4707597	+	IGR	(15)	6.6	6.2	
KpnR_113	Pseudomonas_P26	NC_009648.1	4769689	4769817	+	3' UTR op	(15)	0.0	0.2	
KpnR_114	SroH	NC_009648.1	4782709	4782823	-	IGR	(15)	11.0	4.0	
KpnR_115	aceK-int	NC_009648.1	4810817	4810901	+	IGR	(15)	3.1	4.1	
KpnR_116	malM_3'	NC_009648.1	4844452	4844548	+	3' UTR op	(15)	0.0	10.1	
KpnR_117	pspG_KPN_RS23890_IGR	NC_009648.1	4854487	4854571	+	IGR	this study	77.7	8.6	
KpnR_118	KPN_RS23935_23940_IGR (sRNA 27)	NC_009648.1	4866884	4867205	+	IGR	(14)	36.3	12.4	
KpnR_119	KPN_RS23955_KPN_RS23965_IGR (sRNA 28)	NC_009648.1	4872137	4872383	+	IGR	(14)	13.6	5.6	
KpnR_120	SraL	NC_009648.1	4885978	4886125	-	IGR	(15)	0.7	0.6	
KpnR_121	iolD_3'	NC_009648.1	5113801	5113867	+	3' UTR	this study	43.1	92.2	
KpnR_122	iolE_3'	NC_009648.1	5116601	5116790	+	3' UTR	this study	10.7	16.6	
KpnR_123	repA_tap_IGR	NC_009649.1	5598	5684	-	IGR	this study	0.1	0.4	
KpnR_124	KPN_RS30785_KPN_RS26475_IGR	NC_009649.1	50982	51224	-	IGR	this study	3.3	6.5	
KpnR_125	pcoE_3'	NC_009649.1	71349	71428	-	3' UTR	this study	32.8	15.5	
KpnR_126	KPN_RS26860_KPN_RS29675_IGR	NC_009649.1	124376	124473	-	IGR	this study	0.0	0.0	
KpnR_127	KPN_RS32575_KPN_RS26920_IGR1	NC_009649.1	134020	134087	-	IGR	this study	9.1	7.0	
KpnR_128	KPN_RS32575_KPN_RS26920_IGR2	NC_009649.1	134372	134491	+	IGR	this study	6.0	5.3	
KpnR_129	repA_tap_IGR	NC_009650.1	5597	5684	-	IGR	this study	n.d.	n.d.	
KpnR_130	KPN_RS27500_27505_IGR	NC_009650.1	58478	58578	-	IGR	this study	n.d.	n.d.	
KpnR_131	KPN_RS27570_27575_IGR	NC_009650.1	68576	68685	-	IGR	this study	n.d.	n.d.	
KpnR_132	traX_KPN_RS27770_IGR	NC_009650.1	106802	106912	-	IGR	this study	n.d.	n.d.	
KpnR_133	KPN_RS27800_27805_IGR	NC_009651.1	3977	4078	+	IGR	this study	0.3	0.3	
KpnR_134	KPN_RS28310_KPN_RS28295_IGR	NC_009652.1	3747	3848	-	IGR	this study	n.d.	n.d.	
KpnR_135	FadZ	NC_009648.1	4747195	4747235	-	3' UTR	(13)	n.d.	n.d.	
KpnR_136	MalH	NC_009648.1	4836639	4836835	-	3' UTR	(16)	n.d.	n.d.	
KpnR_137	ZbiJ	NC_009648.1	929321	929471	-	3' UTR	(13)	n.d.	n.d.	

(a) determined for newly annotated sRNA candidates

Supplementary Table S2 – LexA boxes in MGH 78578

reference genome	TSS position	strand	associated gene	alternative name	motif	*E. coli* LexA regulon	Hfq-RIPseq enrichment MEP	Hfq-RIPseq enrichment ESP
NC_009648.1	69500	-	KPN_RS00315	*dinA/polB*	ACCTGTATAAAACCCCAGCG	yes	0,5	0,8
NC_009648.1	134256	+	as in KPN_RS00615		TATTGTAGGTCCACTCAGGA	na	na	na
NC_009648.1	279304	+	KPN_RS01315	*dinB*	TGCTGTATGGGTATACAGTG	yes	0,6	0,9
NC_009648.1	302334	+	KPN_RS01425		TAATTTTTGCACAACCAGCG	no homologue in MG1655	1,0	0,5
NC_009648.1	304001	+	KPN_RS01430		AAATGTTCAATAAATCAGTA	no homologue in MG1655	1,6	0,8
NC_009648.1	495194	-	KPN_RS02385	*priC*	TAATGGTTAAAATAACAGGT	no	0,5	0,5
NC_009648.1	513937	+	KPN_RS02475	*cueR*	TCCTGAATAATTTTCCGGTC	no	0,4	0,6
NC_009648.1	898954	+	KPN_RS04345	*uvrB*	CACTGTTTAAATATCCAGTA	yes	0,5	0,6
NC_009648.1	926126	+	KPN_RS04480	*dinG*	TAGTGGCTGTTTATACAGTA	yes	0,4	0,6
NC_009648.1	938906	-	KPN_RS04540	*rhtA*	CCCTGTTTTTTTCAACATTA	no	0,4	0,8
NC_009648.1	1032191	+	KPN_RS04965	*ftsK*	TCCTGTTAATCCATACAGCA	yes	0,4	0,4
NC_009648.1	1122285	-	KPN_RS05300	*sulA*	TACTGTATATGCATACAGTA	yes	2,8	2,7
NC_009648.1	1222445	-	KPN_RS32185	*dinI*	TACTGTATAAATAACCAGTA	yes	**15,2**	**7,9**
NC_009648.1	1330706	-	KPN_RS06320		CACTGTACATTAATACAGTA	no homologue in MG1655	0,7	0,7
NC_009648.1	1330925	+	KPN_RS06325	*ltrA*	TACTGTATATATATTCAGTG	no homologue in MG1655	0,5	**5,7**
NC_009648.1	1392082	-	KPN_RS06630	*ydjM*	TACTGTATGAATCGACAGTT	yes	0,8	2,1
NC_009648.1	1392082	-	KPN_RS06630	*ydjM*	CACTGTATAAAAACCCTATA	yes	0,8	2,1
NC_009648.1	1580772	+	KPN_RS07645		TTCTGATTGTAATCACAGGA	no homologue in MG1655	1,9	1,6
NC_009648.1	1602046	-	KPN_RS07740	*uspF*	GAAGGGATACTTAAACAGGA	no	1,5	0,5
NC_009648.1	1755352	-	KPN_RS08465	*dmsD*	CAATGGCTACACCACCAGCG	no	0,7	1,9
NC_009648.1	2113961	-	KPN_RS32425		TACTGTTCTTATAATCAATA	no homologue in MG1655	0,7	1,1
NC_009648.1	2116422	-	KPN_RS10330		TACTGTATAAAAAAACAGTA	no homologue in MG1655	0,5	0,8
NC_009648.1	2196973	+	internal in mdtK	*mdtK*	TACTGGTCAACATTCCGGTG	no	2,1	2,7
NC_009648.1	2366135	+	KPN_RS11635	*ydiK*	TATTGATATTATTATCAGTA	no	0,7	0,6
NC_009648.1	2445265	-	KPN_RS12010	*chaC*	AGCTGGATAATATTTCAGCA	no	0,6	0,9
NC_009648.1	2548585	-	KPN_RS12535	*dinG*	CACTGTCCAAATAACCAGGG	yes	0,4	0,6
NC_009648.1	2556314	-	KPN_RS12575	*yoaE*	TTCCGTTTAATTACTCAGGA	no	0,6	0,5
NC_009648.1	2602370	-	KPN_RS12815	*ruvA*	GGCTGGATATCTATCCAGCC	yes	0,4	0,4
NC_009648.1	2619131	-	KPN_RS12900	*otsB*	CACTGTCTATACTTACATGG	yes	0,6	1,0
NC_009648.1	2689997	-	KPN_RS13305	*sbmC*	AGCTGTATATTCATACAGTA	yes	0,5	0,4
NC_009648.1	2714275	-	KPN_RS13395		TACTGGTTTTACTAACCGCT	no homologue in MG1655	1,5	1,3
NC_009648.1	2714275	-	KPN_RS13395		TAATGGTTTTATACACTGGA	no homologue in MG1655	1,5	1,3
NC_009648.1	2803617	+	KPN_RS13750		CACTTTTTAAAAATCCAGTG	no	1,1	**6,7**
NC_009648.1	2867663	-	as in KPN_RS14035		ATCTGGACAATAAAAAAGTT	na	na	na
NC_009648.1	3167027	-	KPN_RS15455	*yfhK/glrK*	TAATGTCATATATATCAGTA	no	0,8	1,2
NC_009648.1	3327869	-	KPN_RS16255	*recA*	TACTGTATGACCATACAGTA	yes	0,6	0,4
NC_009648.1	3350324	+	KPN_RS16375		AACTGGTATTTTATCCAGTA	yes	0,5	0,5
NC_009648.1	3350324	+	KPN_RS16375		ACCTGTTTACAATAACTGGT	yes	0,5	0,5
NC_009648.1	3646387	-	KPN_RS17835	*yqfA*	CACTGGAATCATTCTCAGTT	no	0,5	0,9
NC_009648.1	3803003	-	KPN_RS18625	*mug*	TGCTGTTTTTATAAACAATG	no	0,4	0,6
NC_009648.1	3829108	-	KPN_RS30150		TACTGTATGTTTATACAGTA	no homologue in MG1655	1,4	1,2
NC_009648.1	3893961	+	KPN_RS19135	*yhaK*	ATCTGGCTAACAATACAGCG	no	**11,7**	1,3
NC_009648.1	3904868	-	KPN_RS19195	*agaR*	AAATGAAAGTTATTCCAGGA	no	1,0	1,3
NC_009648.1	4068128	-	KPN_RS20110	*rpsJ*	TGATGATTTTCTAAACAGCA	no	1,0	1,9
NC_009648.1	4113170	+	int in KPN_RS20365		TTCTGATATTCCTTACAGCT	na	na	na
NC_009648.1	4121558	-	KPN_RS20400	*ompR*	AAATGTATACTTAACCTGCT	no	0,5	0,6
NC_009648.1	4170640	-	KPN_RS20610	*phd antitoxin*	TGTTGTACAATAAAAGAGTA	no	na	na
NC_009648.1	4182892	+	KPN_RS20675	*ydcR*	TGTCGTTTATTTACACAGGA	no	na	na
NC_009648.1	4275970	-	KPN_RS21060	*dppA*	CGCTGGATGTAAAACCCGGC	no	na	na

NC_009648.1	4378809	+	KPN_RS21565	*rpoZ*	GACTGAACCCACATTCAGTA	no	0,7	0,9
NC_009648.1	4416113	-	KPN_RS21735	*nlpA*	AGATGATTTTATTTCCAGTT	no	1,1	1,9
NC_009648.1	4463983	+	KPN_RS21985	*tisB*	TACTGTTCATCCATACAGTG	yes	1,3	**4,3**
NC_009648.1	4508691	+	KPN_RS22205		TGCTGTATAATTAACCAGTT	no homologue in MG1655	2,2	1,7
NC_009648.1	4585490	-	KPN_RS22560	*aes*	CACTGGATATTAAAACAGTA	no	0,8	1,3
NC_009648.1	4718603	+	KPN_RS23230	*uvrD*	CTCTGTATATATTAACAGGG	yes	0,8	1,7
NC_009648.1	4726754	-	as in KPN_RS23265	*rhtC*	ATCTGGTAGCCCATCCAGCA	na	na	na
NC_009648.1	4732717	-	KPN_RS23295	*metR*	TACTGTATATTCCTCAAGCG	no	0,8	0,9
NC_009648.1	4737198	+	KPN_RS23315	*rmuC*	AACTGGACGTTTGTACAGCA	yes	0,6	0,5
NC_009648.1	4764396	+	KPN_RS23455	*tRNA-Gly*	TAATGGCTATTACCTCAGCC	no	na	na
NC_009648.1	4849108	+	KPN_RS23845	*lexA*	AACTGTATATACACCCAGGG	yes	1,1	**3,4**
NC_009648.1	4849108	+	KPN_RS23845	*lexA*	AGCTGTATATACTCACAGCA	yes	1,1	**3,4**
NC_009648.1	4864335	-	KPN_RS23925	*uvrA*	TACTGTATATTCATTCAGGT	yes	0,8	0,5
NC_009648.1	4864417	+	KPN_RS23930	*ssb1*	ACCTGAATGAATATACAGTA	yes	0,6	0,5
NC_009648.1	5137712	-	KPN_RS30735		TGCTGTATAAATATACATTA	no homologue in MG1655	2,4	1,1
NC_009648.1	5137763	+	as in KPN_RS25310		TAATGTATATTTATACAGCA	na	na	na
NC_009648.1	5308814	-	KPN_RS26165	*robA*	CACTGAATGCTAAAACATCA	no	0,7	0,8
NC_009649.1	109182	+	KPN_RS26790		ACCTGTATCCATAAACAGTG	no homologue in MG1655	1,0	1,2
NC_009650.1	29810	-	KPN_RS27330		CGCTGTAAAACAAAACAGGC	no homologue in MG1655	na	na
NC_009650.1	50040	-	KPN_RS27430	*umuD*	TACTGTATGCATAACCAGTA	yes	na	na
NC_009651.1	61448	-	KPN_RS28135	*umuD*	TACTGTATGCATAACCAGTA	yes	0,7	0,9
NC_009653.1	525	+	orphan		TGATGTTTAAACTTATAGTG	na	na	na

Supplementary Table S3 – Bacterial strains

strain	stock name	genotype/relevant markers		source/reference
Klebsiella pneumoniae subsp. pneumoniae MGH 78578				
WT	KFKS-031	pKPN3-7	1; 2; 3A/C/D; 4; 6A/B; S1; S2B/C; S3A; S4; S6A; S7; S8A; S9A; S11A/B; S12C/D	(14)
WT	KFKS-245	pKPN3; pKPN5; pKPN7	3E; 6C; S2B; S3B; S6B	this study
Δ***hfq***	KFKS-024	pKPN3; pKPN5; pKPN7; Δ*hfq*	3C/E; S2B/C; S3B	this study
hfq::3xFLAG	KFKS-061	pKPN3; pKPN5; pKPN7; *hfq::3xFLAG*	1; 2; 3A; 4A; S2B/C; S3A; S4; S6A	this study
Δ***dinIR***	KFKS-198	pKPN3; pKPN5; pKPN7; Δ*dinI*	6; S6B; S8A; S12C/D	this study
Δ***dinR***	KFKS-199	pKPN3; pKPN5; pKPN7; Δ*dinR*	6	this study
Δ***sulA***	KFKS-230	pKPN3; pKPN5; pKPN7; Δ*sulA*	6	this study
Δ***dinIR*** Δ***sulA***	KFKS-231	pKPN3; pKPN5; pKPN7; Δ*dinI* Δ*sulA*	6	this study
Δ***dinR*** Δ***sulA***	KFKS-232	pKPN3; pKPN5; pKPN7; Δ*dinR* Δ*sulA*	6	this study
Escherichia coli				
WT	KFS-0088	TOP10 *F- mcrA Δ(mrr-hsdRMS-mcrBC) φ80lacZΔM15 ΔlacX74 nupG recA1 araD139 Δ(ara-leu)7697 galE15 galK16 rpsL(StrR) endA1 λ-*	4B/C/D; 5D/E; S9A; S11C	Invitrogen
	KFS-0033	S17 *ΔlacU169 (ΦlacZΔM15) recA1 endA1 hsdR17 thi-1 gyrA96 relA1 λpir*		New England Biolabs
Vibrio cholerae **O1 El Tor C6706**				
WT	KPS-0014		4B/C/D; S9A	(18)
Salmonella **Typhimurium SL1344**				
rne-ctrl.	JVS-6999	*[rluC-rne]IG::cat*	S6B	(19)
rne**-TS**	JVS-7000	*[rluC-rne]IG::cat rne-3071 (ts)*	S6B	(19)

Supplementary Table S4 – Plasmids

trivial name	plasmid ID	description	origin, marker	used in Figure	reference
$pBAD_{EC}$-*ctrl.*	pKP8-35	empty vector (used in *E. coli*)	pBR322, Amp^R	4B/C/D; 5D/E; S9A; S11C	(9)
pXG10	pXG10-sfGFP	empty vector (used in *E. coli*)	pSC101*, Cm^R		(9)
$pBAD_{KP}$-*ctrl.*	pER41	empty vector (used in *K. pneumoniae*)	pBR322, Apm^R	4B/C/D/E; S8A; S9A; S11A/B	this study
$pBAD_{VC}$-*ctrl.*	pBAD1K-ctrl	empty vector (used in *V. cholerae*)	p15A, Kan^R	4B/C/D; S9A	(20)
pACBSR-hyg		temperature-sensitive plasmid to express λRED-recombinase system from the arabinose-inducible *araBAD* promoter	p15A, Hyg^R		(6)
pFLP-hyg		temperature-sensitive Flp recombinase expression plasmid	p15A, Hyg^R		(6)
pIJ773		template for apramycin resistance (*aac(3)IV*) and flanking FRT sites to construct chromosomal deletions in *K. pneumoniae*	pBR322, Apm^R		(6)
pIJ773-3xFLAG	pER15	template for apramycin resistance (*aac(3)IV*) and flanking FRT sites to construct chromosomal *K. pneumoniae hfq::3xFLAG*	pBR322, Apm^R		this study
$pBAD_{EC}$-DinR	pFS1	expression of DinR under control of the *araBAD* promoter in *E. coli*	pBR322, Amp^R	4B/C/D; 5D/E; S9A; S11C	this study
$pBAD_{KP}$-DinR	pER45	expression of DinR under control of the *araBAD* promoter in *K. pneumoniae*	pBR322, Apm^R	4B/C/D/E; S9A; S11A/B	this study
$pBAD_{VC}$-DinR	pER114	expression of DinR under control of the *araBAD* promoter in *V. cholerae*	p15A, Kan^R	4B/C/D; S9A	this study
ftsZ::gfp	pFS7	expression of *ftsZ::gfp* translational fusion (-62 to /60 of *ftsZ* relative to the translational start site) under control of the $P_{LtetO-1}$ promoter	pSC101*, Cm^R	5D/E	this study
$pBAD_{EC}$-DinR-M3	pER43	expression of DinR-M3 under control of the *araBAD* promoter in *E. coli*	pBR322, Amp^R	5D/E; S11C	this study
$pBAD_{KP}$-DinR-M3	pER84	expression of DinR-M3 under control of the *araBAD* promoter in *K. pneumoniae*	pBR322, Apm^R	S11A/B	this study
ftsZ*-M3*::gfp	pER44	expression of *ftsZ-M3::gfp* translational fusion (-62 to /60 of *ftsZ* relative to the translational start site) under control of the $P_{LtetO-1}$ promoter	pSC101*, Cm^R	5D/E	this study
$pBAD_{EC}$-DinR-M2	pFS51	expression of DinR-M2 under control of the *araBAD* promoter in *E. coli*	pBR322, Amp^R	S11C	this study
$pBAD_{KP}$-DinR-M2	pER85	expression of DinR-M2 under control of the *araBAD* promoter in *K. pneumoniae*	pBR322, Apm^R	S11A/B	this study
$pBAD_{EC}$-DinR-M4	pER65	expression of DinR-M4 under control of the *araBAD* promoter in *E. coli*	pBR322, Amp^R	S11C	this study
$pBAD_{KP}$-DinR-M4	pER89	expression of DinR-M4 under control of the *araBAD* promoter in *K. pneumoniae*	pBR322, Apm^R	S11A/B	this study
$pBAD_{EC}$-DinR-M1	pER66	expression of DinR-M1 under control of the *araBAD* promoter in *E. coli*	pBR322, Amp^R	S11C	this study
$pBAD_{KP}$-DinR-M1	pER90	expression of DinR-M1 under control of the *araBAD* promoter in *K. pneumoniae*	pBR322, Apm^R	S11A/B	this study
$pBAD_{EC}$-DinRshort	pFS54	expression of DinRshort under control of the *araBAD* promoter in *E. coli*	pBR322, Amp^R	S11C	this study
$pBAD_{KP}$-DinRshort	pER95	expression of DinRshort under control of the *araBAD* promoter in *K. pneumoniae*	pBR322, Apm^R	4B/C/D; 5D/E; S9A; S11C	this study
$pBAD_{EC}$.*dinIR*	pER37	expression of *dinIR* under control of the *araBAD* promoter in *E. coli*	pBR322, Amp^R	S11A/B	this study
pTSS_*dinIR*	pER82	expression of *dinIR* transcript from TSS (-22 relative to the translational start site) in *K. pneumoniae*	pBR322, Apm^R	S8B	this study
pPown_*dinIR*	pER83	expression of *dinI*R transcript -47 from TSS (-69 relative to the translational start site) in *K. pneumoniae*; mutation of *dinI* start codon (ATG to AGG)	pBR322, Apm^R	S8A	this study
pPown_*dinI*$_{AGG}$*R*	pER156	expression of *dinI*R transcript -47 from TSS (-69 relative to the translational start site) in *K. pneumoniae*	pBR322, Apm^R	S8A; S12C/D	this study
pPown_*dinIR*$_{M16}$	pER158	expression of *dinI*R transcript -47 from TSS (-69 relative to the translational start site) in *K. pneumoniae;* DinR lacks nt 114-130	pBR322, Apm^R	S12C/D	this study

Supplementary Table S5 – Oligonucleotides

oligo ID	Sequence 5‘ to 3‘	description
oligonucleotides for construction of plasmids		
KFO-1250	GATCATGACATCGATTACAAGGATGACGATGACAAGTAGTAACTGG AGCTGCTTCGAAGTTC	plasmid construction pER15
KFO-1251	GATGTCATGATCTTTATAATCACCGTCATGGTCTTTGTAGTCCCTAC ACATCGAATTCCTGC	plasmid construction pER15
KPO-1702	ATGCATGTGCTCAGTATCTCTATC	linearization pXG10
KPO-1703	GCTAGCGGATCCGCTGG	linearization pXG10
KPO-0196	GGAGAAACAGTAGAGAGTTGCG	linearization pBAD/pBAD1K
KPO-0411	TTTTTCTAGATTAAATCAGAACGC	linearization pBAD; construction pER82/pER83
KPO-1397	GATCCGGTGATTGATTGAGC	linearization pBAD1K
KFO-1713	GAGATACTGAGCACATGCATTTTTTTAAGAGAACGCAGACAATTAG	plasmid construction pFS7
KFO-1714	GAGCCAGCGGATCCGCTAGCGCCACCGACGCCGATG	plasmid construction pFS7
KPO-1715	CAACTCTCTACTGTTTCTCCAAGAAGACAAAGACCGGATAAG	plasmid construction pFS1/ER114
KPO-1716	TCTGATTTAATCTAGAAAAACGATATTGAGCAGAATAATCAGG	plasmid construction pFS1/pER37/pER82/pER83
KFO-1832	ACTCTTCCTTTTTCAATATTATTGAAG	plasmid construction pER41
KFO-1833	CTGTCAGACCAAGTTTACTC	plasmid construction pER41
KFO-1830	AATATTGAAAAAGGAAGAGTATGTCATCAGCGGTGGAG	plasmid construction pER41
KFO-1831	GAGTAAACTTGGTCTGACAGTCAGCCAATCGACTGGCG	plasmid construction pER41
KFO-1787	CAACTCTCTACTGTTTCTCCGTATCGAACGCAGGGGG	plasmid construction pER37
KFO-2027	GGTAACGAATCAGACAATTGAC	plasmid construction ER82/pER83
KFO-2028	GTCAATTGTCTGATTCGTTACCGTATCGAACGCAGGGGG	plasmid construction pER82
KFO-2029	GTCAATTGTCTGATTCGTTACCCGCAGCCCCCTGTTG	plasmid construction pER83
KFO-2140	GCTCAATCAATCACCGGATCCGATATTGAGCAGAATAATCAGG	plasmid construction pER114
oligonucleotides for mutagenesis		
KFO-1849	CATTGTGGTTTTTTTGCCGGGTCGCC	plasmid construction pER43
KFO-1850	CAAAAAAACCACAATGAGGGAGCAAACC	plasmid construction pER43
KFO-1851	CGACAGCCACAAGACGGAGAGAAACTATG	plasmid construction pER44
KFO-1852	CTTGTGGCTGTCGCCTGAGAACGC	plasmid construction pER44
KFO-1892	CCTCATTCTGCTTTTTTTGCCGGGTCG	plasmid construction pFS51
KFO-1893	AAAAGCAGAATGAGGGAGCAAACCAGAG	plasmid construction pFS51
KFO-1898	CGCAACTCTCTACTGTTTCTCCTTACTCTGGTTTGCTCCCTC	plasmid construction pFS54
KPO-0196	GGAGAAACAGTAGAGAGTTGCG	plasmid construction pFS54
KFO-1990	CTTTTTTTCCCGGGTCGCCCCGGC	plasmid construction pER65
KFO-1991	CCCGGGAAAAAAAGCACAATGAGG	plasmid construction pER65
KFO-1992	GTTTGCTGCCTCATTGTGCTTTTTTTG	plasmid construction pER66
KFO-1993	AATGAGGCAGCAAACCAGAGTAACTG	plasmid construction pER66
KFO-2719	GCAATTAGGCGCATTGAAGTGTCTATCG	plasmid construction pER156
KFO-2720	CAATGCGCCTAATTGCCCCCTGCGTTCG	plasmid construction pER156
KFO-2721	TTTTTGCCGGGTCGCCC	plasmid construction pER158
KFO-2723	GGGCGACCCGGCAAAAACAAACCAGAGTAACTGGATCC	plasmid construction pER158
oligonucleotides for Northern blot probing		
KPO-0009	CTACGGCGTTTCACTTCTGAGTTC	oligoprobe 5S rRNA
KPO-0353	GAATTGGGACAACTCCAGTG	oligoprobe *gfp*
KFO-0510	GAATACTGCGCCAACACCAG	oligoprobe ArcZ
KFO-0748	GCCCGTCAAAGAGGAATTTC	oligoprobe ChiX
KFO-1297	CTCGTTCCGGCTCAGGA	oligoprobe GcvB
KFO-1745	GGCAAAAAAAGCACAATGAGGGAGCAAACCAG	oligoprobe DinR
KFO-1853	AGTTTCTCTCCGTCTTGTGC	oligoprobe *ftsZ*
KFO-1973	AATGAGGGAGCAAACCAGAGTAA	oligoprobe DinR
KFO-2239	AAGCAGGCGAACATCACTGG	oligoprobe KpnR_128
KFO-2394	GTACGGGCAATCATCATATTGG	oligoprobe MicL
KFO-2401	CTAAGGAGGTGGTTCCTGG	oligoprobe CyaR
KFO-2423	CGAAGATCAGATCTAAAGTTTGG	oligoprobe KpnR_105
KFO-2551	GTTCGGCTGTATGTAGGGTAC	oligoprobe KpnR_117
oligonucleotides for strain construction		
KFO-1407	TGTAGGCTGGAGCTGCTTC	amplification aac(3)IV::FRT
KFO-1376	CCGGGGATCCGTCGACC	amplification aac(3)IV::FRT
KFO-1375	GACTACAAAGACCATGACGG	amplification aac(3)IV::FRT::3xFLAG
KFO-1252	GATACCGCCAGATGTGGTC	Δ*hfq* and *hfq*::3xFLAG
KFO-1255	AGCGCCGGTCGCTTTAAC	Δ*hfq* and *hfq*::3xFLAG
KFO-1378	GGTCGACGGATCCCCGGGGCCAGTGCTGTTTTTCCAC	Δ*hfq*
KFO-1408	GAAGCAGCTCCAGCCTACAATTCTCTCTTTTCCTTATATGTAT	Δ*hfq*
KFO-1377	CCGTCATGGTCTTTGTAGTCTTCGGCGTCGTCGCTGTC	*hfq*-3xFLAG
KFO-1378	GGTCGACGGATCCCCGGGGCCAGTGCTGTTTTTCCAC	*hfq*-3xFLAG
KFO-1798	GGTCGGACCGTTGTTGTTC	Δ*sulA*

KFO-1799	CAGGCCTTCAGATAAATGTTC	Δ*sulA*
KFO-1800	GGTCGACGGATCCCCGGGTGAAATTAGGATTATTCCTGG	Δ*sulA*
KFO-1801	GAAGCAGCTCCAGCCTACACATAGTCTATGCCGCCTTTAG	Δ*sulA*
KFO-1814	AATATCAAGCTTATCGATACCG	amplification pIJ773
KFO-1815	CATCGAATTCCTGCAGCC	amplification pIJ773
KFO-1792	GCAATGCCTGCTTCCAGG	Δ*dinI* and Δ*dinR*
KFO-1793	GCAGCATCTGATGTTCAACC	Δ*dinI* and Δ*dinR*
KFO-1905	CGAAGCAGCTCCAGCCTACATGGTTATTTATACAGTATCCGG	Δ*dinI*
KFO-1821	GCAGGTCGACGGATCCCCGGATCCCCTCTTCTGTTCAGAATAG	Δ*dinI*
KFO-2000	CGAAGCAGCTCCAGCCTACATCAGGAGAGATCGTGGAC	Δ*dinR*
KFO-2001	GCAGGTCGACGGATCCCCGGCTTTTTTTGCCGGGTCGCC	Δ*dinR*
oligonucleotides for T7 templates		
KFO-1762	GTTTTTTTTAATACGACTCACTATAGGCGACCCGGCAAAAAAAG	fwd DinR riboprobe
KFO-1763	GATAAGCGAAATCCTGCAGG	rev DinR riboprobe
KFO-2288	GTTTTTTTTAATACGACTCACTATAGGCTGGGCAGCGTTAACGAG	fwd *sulA* riboprobe
KFO-2260	CGAATGGGTTCAGTCCGC	rev *sulA* riboprobe
KFO-2554	GTTTTTTTTAATACGACTCACTATAGGACGCTCACCTGGCTATC	fwd *dinI* riboprobe
KFO-2555	CGCATTGAAGTGTCTATCGC	rev *dinI* riboprobe
KFO-1899	GTTTTTTTTAATACGACTCACTATAGGTTACTCTGGTTTGCTCCCTC	fwd T7 template DinRshort
KFO-1900	GTTTTTTTTAATACGACTCACTATAGGAAGAAGACAAAGACCGGATAAG	fwd T7 template DinR
KFO-1691	AAAAAAAGCCGGGGCGACC	rev T7 template DinR/DinRshort
KFO-1902	GTTTTTTTTAATACGACTCACTATAGGTTAAGAGAACGCAGACAATTAG	fwd T7 template *ftsZ*
KFO-1901	GCCACCGACGCCGATG	rev T7 template *ftsZ*
oligonucleotide for primer extension		
KFO-1745	GGCAAAAAAAGCACAATGAGGGAGCAAACCAG	primer extension *dinIR*
oligonucleotides for qPCR (ChIP analysis)		
KFO-2724	GCGATAGACACTTCAATGCG	qPCR P*dinI*
KFO-2725	GTGAAGAAATAAAAACGCAGCC	qPCR P*dinI*
KFO-2726	GTAAAGCGTGTTCGCTTCG	qPCR P*recA*
KFO-2727	CTATGCGCTAAATCTGCTCTG	qPCR P*recA*
KFO-2756	GTATTGCCCTGCAGCGTC	qPCR *sgrR*
KFO-2757	GCTCAAGATCCATGCCTTTG	qPCR *sgrR*
oligonucleotides for rRNA depletion		
23S_1	[Btn]ACCTTTCCCTCACGGTACTGGTTCGCTATCGGTCA	23S rRNA depletion #1
23S_2	[Btn]AGTCGCTGGCTCATTATACAAAAGGTACGCCGTCACC	23S rRNA depletion #2
23S_3	[Btn]TCGGGGAGAACCAGCTATCTCCGGGTTTGATTGGC	23S rRNA depletion #3
23S_4	[Btn]GTGGCTGCTTCTAAGCCAACATCCTG	23S rRNA depletion #4
23S_5	[Btn]GGGTACAGGAATATTAACCTGATTTCCATCGACTACGCC	23S rRNA depletion #5
23S_6	[Btn]CACCTGTGTCGGTTTGGGGTACGGT	23S rRNA depletion #6
23S_7	[Btn]TCGTGCGGGTCGGAACTTACCCGACAAG	23S rRNA depletion #7
23S_8	[Btn]GAGCCGACATCGAGGTGCCAAACA	23S rRNA depletion #8
23S_9	[Btn]CGGCGGATAGGGACCGAACTGTCTCACGAC	23S rRNA depletion #9
16S_1	[Btn]CCGCTCGACTTGCATGTGTTAAGCATGCCGACAGCGTTCG	16S rRNA depletion #1
16S_2	[Btn]CCCATTGTGCAAGATTCCCTACTGCTGCCTCCCGT	16S rRNA depletion #2
16S_3	[Btn]ACCGCGGCTGCTGGCACGGAGT	16S rRNA depletion #3
16S_4	[Btn]ACGGCGTGGACTACCAGGGTAT	16S rRNA depletion #4
16S_5	[Btn]TCCACATGCTCCACCGCTTGTGCGGGCCCCCG	16S rRNA depletion #5
16S_6	[Btn]ACCCAACATCTCACAACACGAGCTGACGACA	16S rRNA depletion #6
16S_7	[Btn]GGGCAGTGTGTACAAGGCCCGGGA	16S rRNA depletion #7
16S_8	[Btn]AAGGAGGTGATCCAGCCGCAG	16S rRNA depletion #8
16S-gram-_1	[Btn]CACGTCCTTCATCGCCTTTTACTGCCAAGGCATCC	16S rRNA depletion - Gram negative bacteria #1
16S-gram-_2	[Btn]CCACACCCGGCCTATCAACGTGGTGGTCTTCGACG	16S rRNA depletion - Gram negative bacteria #2
5S_1	[Btn]GTTCGGGAAGGGGTCAGGTGGGTCCAACGCGCTA	5S rRNA depletion #1
5S_2	[Btn]AGACCCCACACTACCATCGGCGATACGTCG	5S rRNA depletion #2
oligonucleotides for RIL-seq		
3Tr3	P-AGATCGGAAGAGCACACGTCTG-ddC	ligation to the cDNA 3′ end
AR2	TACACGACGCTCTTCCGAT	reverse transcription primer
BC5_adaptor	P-AATCACTTGAGATCGGAAGAGCGTCGTGTA-ddC	ligation to the RNA 3′ end
BC6_adaptor	P-ACCAAGTCGAGATCGGAAGAGCGTCGTGTA-ddC	ligation to the RNA 3′ end
BC7_adaptor	P-ACAACTCGCAGATCGGAAGAGCGTCGTGTA-ddC	ligation to the RNA 3′ end
BC8_adaptor	P-ACCCGTCTTAGATCGGAAGAGCGTCGTGTA-ddC	ligation to the RNA 3′ end
P5_Enr	AATGATACGGCGACCACCGAGATCTACACTCTTTCCCTACACGACGCTCTTCCGATCT	PCR enrichment
P7_BC1_Enr	CAAGCAGAAGACGGCATACGAGATTCGTGTGCGTGACTGGAGTTCAGACGTGTGCTCTTCCGATCT	PCR enrichment

Supplementary References

1. Kim D*, et al.* (2012) Comparative analysis of regulatory elements between Escherichia coli and Klebsiella pneumoniae by genome-wide transcription start site profiling. *PLoS Genet* 8(8):e1002867.
2. Corpet F (1988) Multiple sequence alignment with hierarchical clustering. *Nucleic Acids Res* 16(22):10881-10890.
3. Fernandez De Henestrosa AR*, et al.* (2000) Identification of additional genes belonging to the LexA regulon in Escherichia coli. *Mol Microbiol* 35(6):1560-1572.
4. Wade JT, Reppas NB, Church GM, & Struhl K (2005) Genomic analysis of LexA binding reveals the permissive nature of the Escherichia coli genome and identifies unconventional target sites. *Genes Dev* 19(21):2619-2630.
5. Katoh K, Rozewicki J, & Yamada KD (2019) MAFFT online service: multiple sequence alignment, interactive sequence choice and visualization. *Brief Bioinform* 20(4):1160-1166.
6. Huang TW*, et al.* (2014) Capsule deletion via a lambda-Red knockout system perturbs biofilm formation and fimbriae expression in Klebsiella pneumoniae MGH 78578. *BMC Res Notes* 7:13.
7. Sharma CM, Darfeuille F, Plantinga TH, & Vogel J (2007) A small RNA regulates multiple ABC transporter mRNAs by targeting C/A-rich elements inside and upstream of ribosome-binding sites. *Genes Dev* 21(21):2804-2817.
8. Fröhlich KS, Papenfort K, Fekete A, & Vogel J (2013) A small RNA activates CFA synthase by isoform-specific mRNA stabilization. *EMBO J* 32(22):2963-2979.
9. Papenfort K*, et al.* (2006) σ^E-dependent small RNAs of *Salmonella* respond to membrane stress by accelerating global *omp* mRNA decay. *Mol Microbiol* 62(6):1674-1688.
10. Huber M*, et al.* (2022) An RNA sponge controls quorum sensing dynamics and biofilm formation in Vibrio cholerae. *Nat Commun* 13(1):7585.
11. Culviner PH, Guegler CK, & Laub MT (2020) A Simple, Cost-Effective, and Robust Method for rRNA Depletion in RNA-Sequencing Studies. *mBio* 11(2).
12. Siemers M, Lippegaus A, & Papenfort K (2023) ChimericFragments: Computation, analysis, and visualization of global RNA networks. *bioRxiv* DOI: 10.1101/2023.12.21.572723.
13. Bar A, Argaman L, Altuvia Y, & Margalit H (2021) Prediction of Novel Bacterial Small RNAs From RIL-Seq RNA-RNA Interaction Data. *Front Microbiol* 12:635070.
14. Bruchmann S*, et al.* (2015) Deep transcriptome profiling of clinical Klebsiella pneumoniae isolates reveals strain and sequence type-specific adaptation. *Environ Microbiol* 17(11):4690-4710.
15. Hör J, Matera G, Vogel J, Gottesman S, & Storz G (2020) Trans-Acting Small RNAs and Their Effects on Gene Expression in Escherichia coli and Salmonella enterica. *EcoSal Plus* 9(1).
16. Iosub IA*, et al.* (2021) The mRNA derived MalH sRNA contributes to alternative carbon source utilization by tuning maltoporin expression in E. coli. *RNA Biol* 18(6):914-931.
17. Bailey TL & Elkan C (1994) Fitting a mixture model by expectation maximization to discover motifs in biopolymers. *Proc Int Conf Intell Syst Mol Biol* 2:28-36.
18. Thelin KH & Taylor RK (1996) Toxin-coregulated pilus, but not mannose-sensitive hemagglutinin, is required for colonization by Vibrio cholerae O1 El Tor biotype and O139 strains. *Infect Immun* 64(7):2853-2856.
19. Figueroa-Bossi N, Valentini M, Malleret L, & Bossi L (2009) Caught at its own game: regulatory small RNA inactivated by an inducible transcript mimicking its target. *Gene Dev* 23(17):2004-2015.
20. Hoyos M, Huber M, Forstner KU, & Papenfort K (2020) Gene autoregulation by 3' UTR-derived bacterial small RNAs. *Elife* 9.